Master thesis

Study of out of equilibrium dynamics of a Josephson Junction array

Supervised by Professor Thierry Giamarchi

Giacomo Morpurgo

August 31, 2020

Acknowledgements

First and foremost, I deeply thank my supervisor Thierry Giamarchi for the possibility of doing my master thesis in his group. It was a wonderful experience to work in this environment. I also want to thank Nirvana Caballero for the great help she gave me when I had to deal with the numeric treatment of our problem. I also thank Christophe Berthod for his help in the discovery of how to use Mafalda and Asymptote.

Special thanks go also to Francesca Ferlaino and her group of the university of Innsbruck, with whom we worked on part of this project. They realized all the experiments and ground state simulations which we used in the second part this work.

I would also thank all the members of the groups for the great environment in which I evolved this year. A special thanks goes to Michele Filippone and Charles Bardyn who shared their office with me, provided me with support and advices as well as some pearls of humour, all of which were extremely welcome. Finally, I would like to thank my parents for their support during these last years.

Contents

Chapter 1

Introduction/Context of the problem

Out of equilibrium physics is a really interesting kind of phenomenon to look at. When a system is coupled to a large reservoir, usually that reservoir allows the system to reach thermal equilibrium by exchanging of particles or energy. That poses the question of how does the system behaves when it is not yet in the thermal equilibrium, what are the dynamics of the system when we push it away from the thermal equilibrium? Another type of question would be to look at how an isolated system evolves. Even if it is not coupled to a reservoir, will it reach an apparent thermal equilibrium state or have a completely different behaviour? One of the examples of this is many-body localization, where systems with a strong disorder do not thermalize.[1]

A standard protocol to study out of equilibrium physics consist in quenching the system. This means suddenly changing the hamiltonian with which the system evolves and look at the reaction of the system.

A good type of systems for investigating these properties are ultracold atomic gases. This is because they are generally well isolated, but also because the quantum evolution happens on timescales which are accessible to experiments and these systems offer a great control on a large number of parameters, which lead to the realization of a great number of different physical systems. For example, one can with optical lattices tune the strength of the tunneling between sites by increasing/decreasing the well depth of the optical lattice.[2]

In this general context, we will in this work look at the effects of quenches of the Josephson coupling parameter in a 1D Josephson junction array model for bosons. The master thesis is organized as following :

- Chapter 1 is a general introduction to the thematics of this master thesis.
- Chapter 2 presents the model that we will study, the Josephson Junction array model and presents also the procedure that we will make our Josephson Junction array go under.
- Chapter 3 contains the first limit that we study in this work : zero temperature and a quantum treatment. We will present the analytical tools that we use to tackle the problem

and we will then discuss the effects of the different parameters of the model.

- Chapter 4 is about the second limit that we study : finite temperature and classical treatment. We will present the Langevin formalism and use it to solve our problem both numerically and analytically.

- In Chapter 5, we apply our model to a precise experiment done with cold dipolar atoms. We will discuss the effects of the parameters of our Josephson Juction array model in the Langevin formalism and use this to see if a Josephson Junction array describes well the experiment.

- Chapter 6 contains the conclusion of this master thesis and also some future works which could be done.

Chapter 2

Introduction to the model (Josephson junction's arrays)

1 Josephson Junction array

1.1 What is a Josephson junction ?

A Josephson junction consists of 2 superconductors separated by a thin non superconducting layer, as can be seen in Fig. 2.1. Each superconductor is characterized by an order parameter which has a given phase and therefore breaks the phase symmetry. In this situation, Cooper pairs may tunnel between the two superconductors, thus creating a current which depends on the difference of phase between the two superconductors. This process was discovered by Josephson, hence the name.[3]

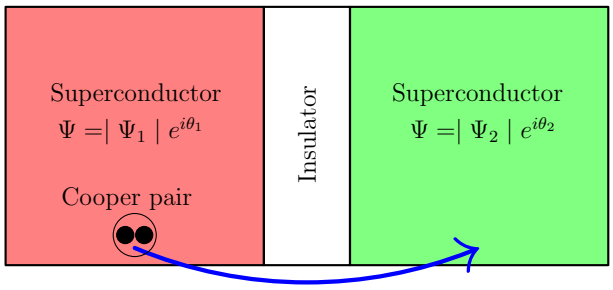

Figure 2.1 – A schematic representing a Josephson Junction. We have two superconductors (their order parameter has a given phase) which are connected by tunneling of Cooper pairs.

1.2 Conjugate variables in superconductors/Josephson Junctions

An important element about superconductors, that we will use profusely in Section 3 is the fact that it is impossible to know precisely and simultaneously the phase and the number of Cooper pairs of any superconductor. This can be seen by looking at the ground state. The BCS "standard" ground state which is : $|BCS, \theta\rangle = \prod_{\mathbf{k}}(u_{\mathbf{k}} + v_{\mathbf{k}} e^{-i2\theta} c^{\dagger}_{\mathbf{k},\uparrow} c^{\dagger}_{-\mathbf{k},\downarrow}) |0\rangle$. This is not a particle number eigenstate, because if we develop the product, one can see that it is a superposition of 0,2,4,... particles states. On the other hand, Anderson managed to write the ground state of the BCS where the number of particles is constant : $|BCS, N_o\rangle = \frac{1}{2\pi} \int_0^{2\pi} d\theta e^{iN_o\theta} |BCS, \theta\}\rangle$ and in this case, because of the integral over the phases, the phase is totally undetermined. So here

we have a sort of uncertainty principle, where we cannot know exactly the number of particles in a superconductor and the phase of the superconducting wave function at the same time. We also get a commutation relation (as for the position and momentum operators).[4]

$$[\theta, N] = i \tag{2.1}$$

1.3 Josephson junction array (JJA)

One can imagine putting several of these junctions in series, as in Fig.2.2. This system is called a Josephson junction array. They can be realized with different dimensionalities : 1d array, 2d arrays or 3d arrays.[5] In our case, we are interested in 1d arrays, so let us focus on it.

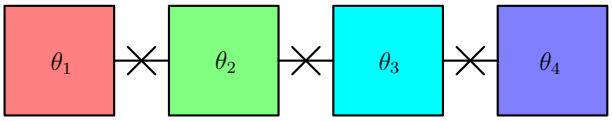

Figure 2.2 – Schematic representing a Josephson junction array. The boxes are the superconductors with a given phase θ_i. The lines with the crosses represent the junctions.

1.3.1 Hamiltonian of a JJA

The Hamiltonian which describes a Josephson junction 1d-array of N sites with periodic boundary conditions is given by (2.2):

$$H = \sum_{i=1}^{N} \frac{(Q_i - Q_{oi})^2}{2C_i} - \sum_{i=1}^{N} J_{i+1,i} \cos(\theta_{i+1} - \theta_i) \tag{2.2}$$

Here, N is the number of sites and each site has a certain amount of charge Q_i, the amount of charge that the site would like to have (costs less energy) Q_{oi}, and a phase θ_i. Furthermore, C_i is the capacitance associated to each site, it tells us how much energy we have to pay if we want to add one Cooper pair to the site. Finally, $J_{i+1,i}$ is the interaction strength between site $i+1$ and i.

To simplify the problem, we consider that each site is the same $\Rightarrow Q_{oi} = Q_o$ and $C_i = C$. Another simplification that we do is also consider each link to be the same : $J_{i+1,i} = J$. We also call $Q_i - Q_{oi} = \delta Q_i$, which are the fluctuations of the charge on site i. The Hamiltonian then becomes :

$$H = \sum_{i=1}^{N} \frac{\delta Q_i^2}{2C} - \sum_{i=1}^{N} J \cos(\theta_{i+1} - \theta_i) \tag{2.3}$$

Here, on each site, we have the commutation relation coming from (2.1). We then get $[\theta_i, N_j] = i\delta_{i,j}$

2 Link to Bose-Hubbard model

One can directly map the Josephson junction array to a Bose-Hubbard model, which also gives some insight to the link between the JJA hamiltonian and the behaviour of the bosons who can jump from a site to the next. Let us take a 1-d array of sites, with jumping coefficient t and interaction U as in Fig.2.3.

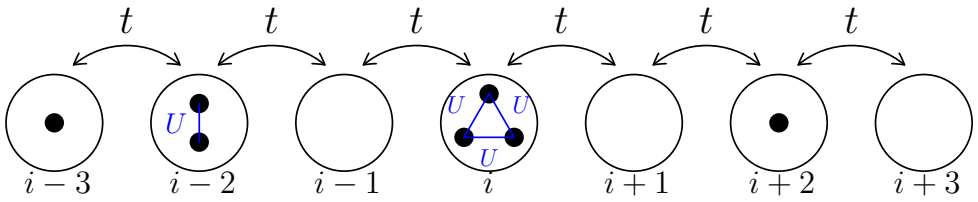

Figure 2.3 – Schematic of the Bose-Hubbard system. Each site can contain an infinite amount of bosons, bosons can tunnel to neighbouring sites with a coefficient t, and there is a cost of energy U for each pair of bosons to be on the same site. On this sketch, the black dots are the bosons and the circles are the different sites.

The hamiltonian is in this case :

$$H = -t\sum_i (c_i^\dagger c_{i+1} + c_{i+1}^\dagger c_i) + \frac{U}{2}\sum_i N_i(N_i - 1) - \mu\sum_i N_i \tag{2.4}$$

where $N_i = c_i^\dagger c_i$. The system gains energy by making the bosons jump between sites (the t-terms), while there is an on-site repulsion U. μ is the chemical potential which fixes an ideal number of particles per site.

If we write the field c_i in terms of its phase and amplitude, $c_i = \sqrt{N_i}e^{i\theta_i}$, we end up with : [6]

$$H = -t\sum_i (\sqrt{N_i}e^{-i\theta_i}\sqrt{N_{i+1}}e^{i\theta_{i+1}} + \sqrt{N_{i+1}}e^{-i\theta_{i+1}}\sqrt{N_i}e^{i\theta_i}) + \frac{U}{2}\sum_i N_i(N_i - 1) - \mu\sum_i N_i \tag{2.5}$$

We can simplify a bit the expression :

$$H = \sum_i (-2t\sqrt{N_i N_{i+1}})\cos(\theta_{i+1} - \theta_i) + \frac{U}{2}\sum_i N_i(N_i - 1) - \mu\sum_i N_i \tag{2.6}$$

We now replace the operator N by its average N_o. Then, in the first term, by identifying the factor $2t\sqrt{N_{o,i}N_{o,i+1}} = J_{i+1,i}$, we have the interaction part of our JJA hamiltonian which is the same as in (2.2). Let us focus on the other part in the case of no tunneling. The chemical potential has the value that minimizes the energy by variation of the number of particles. By assuming $N_{o,i} \gg 1$, we end up with $\mu = UN_{o,i}$. If we now look at fluctuations around this value, $N_i = N_{io} + \delta N_i$ and use the no-tunneling ground state value for the chemical potential, we end up with :

$$\frac{U}{2}\sum_i (N_{io}^2 + 2\delta N_i N_{io} + \delta N_i^2) - U\sum_i (N_{io}^2 + N_{io}\delta N_i) \tag{2.7}$$

And then :

$$-\frac{U}{2}\sum_i N_{io}^2 + \frac{U}{2}\sum_i \delta N_i^2 \tag{2.8}$$

The term in N_{io} is a constant and therefore we can get rid of it in the Hamiltonian as long as we don't compute absolute energies. If we put it back with also a tunneling term, we end up with :

$$H = -\sum_i J_{i+1,i}\cos(\theta_{i+1} - \theta_i) + \frac{U}{2}\sum_i \delta N_i^2 \tag{2.9}$$

and if we identify $U = \frac{1}{C}$, we get back the JJA Hamiltonian, where we replaced the charge Q by the number of atoms N.

3 Time evolution protocol of the system

In the following chapters, we will look at the situation where our system starts in the ground state of a JJA hamiltonian with a given coupling J_2. The state of the system does not change because it is an eigenvector of the Hamiltonian. We then quench the coupling J to a smaller value J_1 at a time t_0 and let the system evolve with less interaction between the sites for a time t_1 and finally we restore the coupling to its original value by quenching it back and look how the phases evolve. Fig.2.4 shows a sketch of the evolution of J in time.

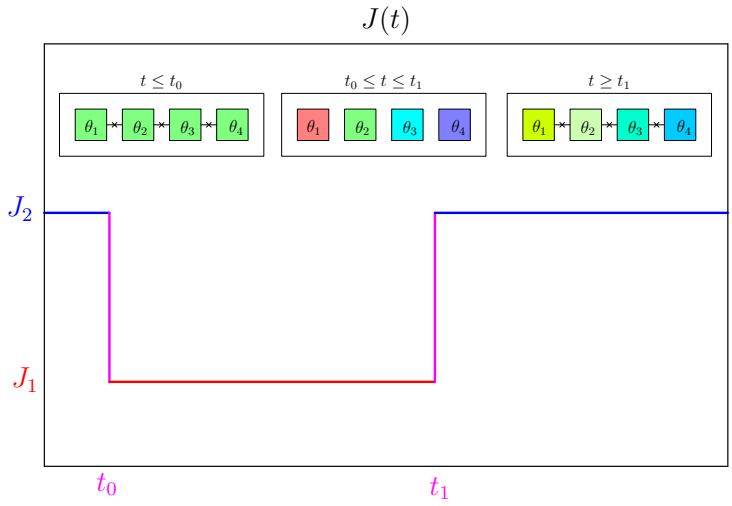

Figure 2.4 – Plot of the value of J as a function of time of our protocol. The inserts show the state of an array of 3 Josephson junctions and 4 superconductors/boxes under our protocol. The phases of the superconductors are characterized by the colors of the boxes. At first, when everything is connected, there is a global phase coherence. When we lower the coupling, the phases can evolve independently on each site and what happens when we put the coupling back is the main question that we want to address.

The idea of what happens is that when we have the smaller coupling, each site evolves independently due to thermal and quantum fluctuations and the phase coherence between the sites is lost (more or less depending on the value of the lower coupling). When we put back the original coupling, the system would like to regain a phase coherence. Does this happens, and if yes, to which degree? It is not clear yet, because the changes of the coupling are mainly quenches (which can be brutal out of equilibrium procedures). It depends also if there is a thermal bath to which the system could dissipate some energy coming from the quench.

We will study this system in two very different limits. In chapter 3, we will be using a quantum formalism at temperature $T = 0$ K, while in chapter 4, we will have the temperature implemented in a Langevin formalism (therefore a classic formalism). In the first limit, when we look at a system with a very long array (a large number of site), it is close to a Luttinger liquid. Similar systems with Luttinger liquids coupled by tunneling which are quenched have been studied both theoretically and experimentally.[7],[8],[9],[10]. There have also been studies directly in the Bose-Hubbard formalism.[11] As we will see in chapter 5, the second limit can be implemented in a way to be compared to experiments done on supersolid phases of cold dipolar atom gases.[12]

Chapter 3

Full quantum approach

In this chapter, we look at the limit of our problem where $T = 0$, with periodic boundaries conditions. But first let us look at what is the main idea of the solution.

1 Idea and technology

We need several things in order to solve this problem. We have to define which observables we want to look at, we have to diagonalize the Hamiltonian in order to easily look at the time evolution of the system and compute the observables. Let us start with the diagonalization of the Hamiltonian.

1.1 Hamiltonian and approximations

Let us look at a system consisting of a 1d ring of sites separated by a distance a which have each a given number of bosons N_i and a phase θ_i.

The Hamiltonian of this system is given by (2.3). The only difference is that here the charge is the number of bosons on the site. We therefore change the notation form Q to N. Be careful that we keep the notation C for the capacitance but here, the notion of capacitance has nothing to do with an electrical charge. It describes the cost of energy one has to make to add an atom to the site. We also replace N_i by $n_i a$, where n_i is the density of particles at the site i.

Our main approximation is that we assume $\theta_{i+1} - \theta_i$ to be small and expand the cosine up to second order. This leads to a quadratic hamiltonian which is analytically solvable. We drop the term JN which changes only the energy level but doesn't intervene in the computation of the observables we will look at.

If we also denote the phases not as absolute but as fluctuations around a reference value, and we take this reference phase to be the same for all sites, we can replace the phase θ_i by the fluctuations of the phases on this site $\delta\theta_i$. Then, our Hamiltonian is :

$$H = \sum_{i=1}^{N} \frac{\delta n_i^2 a^2}{2C} + \sum_{i=1}^{N} \frac{J}{2}(\delta\theta_{i+1} - \delta\theta_i)^2 \tag{3.1}$$

Now the first step is to use a transformation of the operators in the Hamiltonian to have it in a diagonal form, which will allow us to compute easily our observables.

1.2 Diagonalization

In this case, because we have a translation invariance, we know that a Fourier transformation will lead us to a diagonal form. Our transformation is :

$$\begin{cases} \delta n_i = \frac{1}{\sqrt{N}} \sum_k \exp(ikr_i)\delta n_k & \delta n_k = \frac{1}{\sqrt{N}} \sum_i \exp(-ikr_i)\delta n_i \\ \delta \theta_i = \frac{1}{\sqrt{N}} \sum_k \exp(ikr_i)\delta \theta_k & \delta \theta_k = \frac{1}{\sqrt{N}} \sum_i \exp(-ikr_i)\delta \theta_i \end{cases} \tag{3.2}$$

where N is the number of sites of the ring.

1.2.1 Quantisation of k

Because we have a finite number of sites, the possible number of values k is finite. Furthermore, the site i is the same as the site $i + N$ because we are on a ring. We have that in the Fourier decomposition :

$$\begin{aligned} e^{ikr_j} &= e^{ikr_{j+N}} \\ e^{ikaj} &= e^{ika(j+N)} \\ 1 &= e^{ikaN} \end{aligned} \tag{3.3}$$

We then get the quantisation of k to be :

$$k = \frac{2\pi}{Na}p, \quad p \in [\![0, N-1]\!] \quad \text{or} \quad p \in [\![-\frac{N-1}{2}, \frac{N-1}{2}]\!] \text{ if N is odd.} \tag{3.4}$$

1.2.2 Return to diagonalisation

With these transformations, our Hamiltonian can be written as :

$$\sum_k \frac{a^2}{2C}\delta n_k^\dagger \delta n_k + \sum_k J(1 - \cos(ka))\delta\theta_k^\dagger \delta\theta_k \tag{3.5}$$

and we also have the commutation relations :

$$\begin{cases} [\delta n_k, \delta\theta_{k'}^\dagger] = -\frac{i}{a}\delta_{k,k'} \\ [\delta n_k, \delta n_{k'}^\dagger] = 0 \\ [\delta\theta_k, \delta\theta_{k'}^\dagger] = 0 \end{cases} \tag{3.6}$$

Now, the idea is to find a transformation of δn, $\delta\theta$ in creation/destruction operators, in such a way that b is an annihilation operator, and therefore $[b_k, b_{k'}^\dagger] = \delta_{k,k'}$. The idea is to try to write the Hamiltonian in a very simple form : $H = \sum_k E_k b_k^\dagger b_k$. To do this, we use the fact that our Hamiltonian is directly mappable to a serie of Harmonic oscillators. We identify δn_k and $\delta\theta_k$ to the operators $\hat{p}$ and $\hat{x}$ of the harmonic oscillator and use the same transformation which leads (for the harmonic oscilator) to the diagonalized Hamiltonian $H = \hbar\omega(\frac{1}{2} + \sum_k a_k^\dagger a_k)$. The

details of the diagonalization of the quantum harmonic oscillator are given in the Appendix A.1.

In our case, we identify $\delta\theta_k$ to $\hat{x}$ and $a\delta n_k$ to $\hat{p}$. We then identify $\frac{1}{C}$ to m and $\frac{2J(1-\cos(ka))}{C}$ to ω^2. We have to identify $a\delta n_k$ to $\hat{p}$ because we want to get rid of the factor $\frac{1}{a}$ in the commutation relation (3.6) to have a perfect correspondence with the harmonic oscillator.

By transposing the definition of the creation operators (A.2) to our situation, we obtain :

$$\begin{cases} b_k = \frac{1}{\sqrt{2}}(\sqrt[4]{2JC(1-\cos(ka))}\delta\theta_k + i\frac{a}{\sqrt[4]{2JC(1-\cos(ka))}}\delta n_k) \\ b_k^\dagger = \frac{1}{\sqrt{2}}(\sqrt[4]{2JC(1-\cos(ka))}\delta\theta_k^\dagger - i\frac{a}{\sqrt[4]{2JC(1-\cos(ka))}}\delta n_k^\dagger) \\ \delta\theta_k = \frac{1}{\sqrt{2}}\frac{1}{\sqrt[4]{2JC(1-\cos(ka))}}(b_k + b_{-k}^\dagger) \\ \delta n_k = -\frac{i}{\sqrt{2}}\frac{\sqrt[4]{2JC(1-\cos(ka))}}{a}(b_k - b_{-k}^\dagger) \end{cases} \tag{3.7}$$

One can easily check that indeed :

$$[b_k, b_{k'}^\dagger] = \delta_{k,k'} \tag{3.8}$$

We have the terms $\delta n_k^\dagger \delta n_k$ and $\delta\theta_k^\dagger\delta\theta_k$ in our hamiltonian. Let us compute them.

$$\begin{cases} \delta n_k^\dagger \delta n_k = \frac{1}{2}\frac{\sqrt{2JC(1-\cos(ka))}}{a^2}(b_k^\dagger b_k - b_k^\dagger b_{-k}^\dagger - b_{-k}b_k + b_{-k}b_{-k}^\dagger) \\ \delta\theta_k^\dagger\delta\theta_k = \frac{1}{2}\frac{1}{\sqrt{2JC(1-\cos(ka))}}(b_k^\dagger b_k + b_k^\dagger b_{-k}^\dagger + b_{-k}b_k + b_{-k}b_{-k}^\dagger) \end{cases} \tag{3.9}$$

And finally, the Hamiltonian, after simplification is indeed diagonal :

$$H = \sum_k \frac{1}{2}\sqrt{\frac{2J}{C}(1-\cos(ka))}(b_k^\dagger b_k + b_{-k}b_{-k}^\dagger) \tag{3.10}$$

We can rename the indices in one part of the sum to get :

$$H = \sum_k \frac{1}{2}\sqrt{\frac{2J}{C}(1-\cos(ka))}(b_k^\dagger b_k + b_k b_k^\dagger) \tag{3.11}$$

1.3 Procedure and observables

Now that we have our Hamiltonian in a diagonal form, it is time to look at exactly what quench protocol we want to study and what we want to compute.

1.3.1 Protocol

Following the idea given in section 2.3, the quench protocol that we follow consists to start with the ground state of the system with a given J_2, which is $|\Psi(0)\rangle = |\varnothing\rangle_b$ where $b_k|\varnothing\rangle_b = 0$. We then let the system evolve for a time t_1 with an Hamiltonian where we changed the value of J, $(J = J_1)$, that we chose such that $J_1 \ll J_2$. As told before, this consists in decreasing (more or less dramatically depending on the numerical values) the tunneling between each site and letting each site evolve independently. We then requench the system and let it evolve up to a time t_2

with the original J_2, which means that we increase again the tunneling between the different sites to its original value.

1.3.2 Observables

The wave function of the system at time t_2 is given by :

$$|\Psi(t_2)\rangle = e^{-iH_{J_2}t_2}e^{-iH_{J_1}t_1}\,|\varnothing\rangle_b \tag{3.12}$$

where the small b indicates that it this state is the ground state for H_{J_2}, and it is destroyed by b operators.

An interesting observable is the correlation between the phase fluctuations at two different sites :

$$\langle\Psi(t)|\,(\delta\theta_{j_1} - \delta\theta_{j_2})^2\,|\Psi(t)\rangle \tag{3.13}$$

If this correlation is 0, it means that the phases are exactly the same at these two sites, and if this is true for some time, the phases are completely locked.
We will look at this observable at different times : at $t = 0$ before the first quench, at t_1 (when we only did one quench) and at t_2 when we will have done the full procedure.

The idea is to express the operators $\delta\theta$ in terms of the operators $b_k, b_k^\dagger$. The main catch is that we have two different Hamiltonians, therefore two families of $b_k, b_k^\dagger$ and we have to find the relation between them to solve our problem.

2 Computing the observables and discussion

2.1 Relations between operators of families a and b

As discussed before we have to deal with 2 different Hamiltonians, the one with J_1 and the one with J_2. We denote the creation/destruction operators of the J_1 Hamiltonian by $a^\dagger, a$ and the creation/destruction operators of the J_2 Hamiltonian by $b^\dagger, b$. We note that because our quench procedure only affects J, the capacitance C is the same for both Hamiltonians.

Looking at both δn_k and $\delta\theta_k$, we work out the relations between the families of operators a and b. We have :

$$\begin{cases} \dfrac{1}{\sqrt{2}}\dfrac{1}{\sqrt[4]{2J_1C(1-\cos(ka))}}(a_k + a_{-k}^\dagger) = \delta\theta_k = \dfrac{1}{\sqrt{2}}\dfrac{1}{\sqrt[4]{2J_2C(1-\cos(ka))}}(b_k + b_{-k}^\dagger) \\ -\dfrac{i}{2}\dfrac{\sqrt[4]{2J_1C(1-\cos(ka))}}{a}(a_k - a_{-k}^\dagger) = \delta n_k = -\dfrac{i}{2}\dfrac{\sqrt[4]{2J_2C(1-\cos(ka))}}{a}(b_k - b_{-k}^\dagger) \end{cases} \tag{3.14}$$

And by simplifying all the common factors, we get :

$$\begin{cases} \dfrac{1}{\sqrt[4]{J_1}}(a_k + a_{-k}^\dagger) = \dfrac{1}{\sqrt[4]{J_2}}(b_k + b_{-k}^\dagger) \\ \sqrt[4]{J_1}(a_k - a_{-k}^\dagger) = \sqrt[4]{J_2}(b_k - b_{-k}^\dagger) \end{cases} \tag{3.15}$$

By playing a bit with this system, we get the relations we were looking for, which are :

$$\begin{cases} a_k = \frac{1}{2}\left(\sqrt[4]{\frac{J_2}{J_1}} + \sqrt[4]{\frac{J_1}{J_2}}\right) b_k + \frac{1}{2}\left(\sqrt[4]{\frac{J_1}{J_2}} - \sqrt[4]{\frac{J_2}{J_1}}\right) b^\dagger_{-k} \\ b_k = \frac{1}{2}\left(\sqrt[4]{\frac{J_2}{J_1}} + \sqrt[4]{\frac{J_1}{J_2}}\right) a_k + \frac{1}{2}\left(\sqrt[4]{\frac{J_2}{J_1}} - \sqrt[4]{\frac{J_1}{J_2}}\right) a^\dagger_{-k} \end{cases} \tag{3.16}$$

2.2 Computing observables

2.2.1 Sanity check $t_2 = 0$, $t_1 = 0$

For a sanity check and to test the computing procedure with a simple case, we start by computing our observable at time 0, when the system hasn't evolved yet with any of the 2 Hamiltonians, but is in the ground state of the Hamiltonian containing J_2.

From (3.13), we want to compute :

$$\langle \varnothing |_b \, (\delta\theta_{j_1} - \delta\theta_{j_2})^2 \, | \varnothing \rangle_b \tag{3.17}$$

To achieve this, we use the Fourier transform of $\delta\theta_i$ and δn_i (3.2). We then get that :

$$\begin{aligned} (\delta\theta_{j_1} - \delta\theta_{j_2})^2 &= \frac{1}{N}\sum_k (e^{ikr_{j_1}} - e^{ikr_{j_2}})\delta\theta_k \sum_{k'} (e^{ik'r_{j_1}} - e^{ik'r_{j_2}})\delta\theta'_k \\ &= \frac{1}{N}\sum_{k,k'} e^{ikr_{j_1}}(1 - e^{ik(r_{j_2}-r_{j_1})}) e^{ik'r_{j_1}}(1 - e^{ik'(r_{j_2}-r_{j_1})})\delta\theta_k\delta\theta'_k \\ &= \frac{1}{N}\sum_{k,k'} e^{i(k+k')r_{j_1}}(1 - e^{ik(r_{j_2}-r_{j_1})})(1 - e^{ik'(r_{j_2}-r_{j_1})})\delta\theta_k\delta\theta'_k \end{aligned} \tag{3.18}$$

We see now that in order to get $\langle \varnothing |_b \, (\delta\theta_{j_1} - \delta\theta_{j_2})^2 \, | \varnothing \rangle_b$, we need first to compute $\langle \varnothing |_b \, \delta\theta_k \delta\theta_{k'} \, | \varnothing \rangle_b$ (all the others terms are numbers and not operators, so they get out of the quantum average) and this is the same for all times, whenever it is 0, t_1 or t_2!

Let's compute then $\langle \varnothing |_b \, \delta\theta_k \delta\theta_{k'} \, | \varnothing \rangle_b$. First we use the definition of $\delta\theta_k$ in terms of b operators (3.7). By calling the prefactor before the operators $B_k = \frac{1}{\sqrt{2}} \frac{1}{\sqrt[4]{2J_2C(1-\cos(ka))}}$, we get :

$$\begin{aligned} \langle \varnothing |_b \, \delta\theta_k \delta\theta_{k'} \, | \varnothing \rangle_b &= B_k B_{k'} \langle \varnothing |_b \, (b_k + b^\dagger_{-k})(b_{k'} + b^\dagger_{-k'}) \, | \varnothing \rangle_b \\ &= B_k B_{k'} \langle \varnothing |_b \, b_k b^\dagger_{-k'} \, | \varnothing \rangle_b \\ &= B_k B_{k'} \delta_{k,-k'} \\ &= \frac{1}{2} \frac{1}{\sqrt{2J_2C(1-\cos(ka))}} \delta_{k,-k'} \end{aligned} \tag{3.19}$$

where we first used the fact that if we have to go from "vacuum" to "vacuum", the only combination of creator/destructions operators which is possible is to first create and then destroy a particle. Then, we used the commutation relation of the b operators (3.8). And finally, we used the fact that the expression of B_k is even in k, therefore $B_k = B_{-k}$.

This result is quite reasonable, because when we take the limit of small k, we can expand the cosine and end up with the same result as we would get in a Luttinger liquid where we would

get $\nabla\theta$ instead of $\theta_i - \theta_j$ which indeed corresponds to the small k limit.[13]

We now can slowly get back to the expression that we wanted to look at. Indeed, we get :

$$\begin{aligned}
\langle\varnothing|_b (\delta\theta_{j_1} - \delta\theta_{j_2})^2 |\varnothing\rangle_b &= \frac{1}{N}\sum_{k,k'} e^{i(k+k')r_{j_1}}(1-e^{ik(r_{j_2}-r_{j_1})})(1-e^{ik'(r_{j_2}-r_{j_1})})\langle\varnothing|_b \delta\theta_k\delta\theta'_k |\varnothing\rangle_b \\
&= \frac{1}{N}\sum_{k,k'} e^{i(k+k')r_{j_1}}(1-e^{ik(r_{j_2}-r_{j_1})})(1-e^{ik'(r_{j_2}-r_{j_1})})\frac{1}{2}\frac{1}{\sqrt{2J_2C(1-\cos(ka))}}\delta_{k,-k'} \\
&= \frac{1}{N}\sum_{k}(1-e^{ik(r_{j_2}-r_{j_1})})(1-e^{-ik(r_{j_2}-r_{j_1})})\frac{1}{2}\frac{1}{\sqrt{2J_2C(1-\cos(ka))}} \\
&= \frac{1}{N}\sum_{k}(2-2\cos(k(r_{j_2}-r_{j_1}))\frac{1}{2}\frac{1}{\sqrt{2J_2C(1-\cos(ka))}} \\
&= \frac{1}{N\sqrt{2J_2C}}\sum_{k}\frac{1-\cos(k(r_{j_2}-r_{j_1})}{\sqrt{1-\cos(ka)}}
\end{aligned} \tag{3.20}$$

where we first used the Kronecker delta to get rid of one of the sums and then used the definition of the cosinus to simplify the expression.

We now have a way to benchmark our next computations with the time evolution.

2.2.2 What happens at time t_1?

Here, we look at the state of the system at time t_1. This allows us to see the effect of the evolution of the system after a change of the Hamiltonian and allows us to benchmark even further our computation.

We know the procedure : compute $\langle\Psi(t_1)|\,\delta\theta_k\delta\theta_{k'}\,|\Psi(t_1)\rangle$, and then $\langle\Psi(t_1)|\,(\delta\theta_{j_1}-\delta\theta_{j_2})^2\,|\Psi(t_1)\rangle$. Let us start.

We have :

$$\begin{aligned}
\langle\Psi(t_1)|\,\delta\theta_k\delta\theta_{k'}\,|\Psi(t_1)\rangle &= \langle\varnothing|_b\, e^{iH_{J_1}t_1}\delta\theta_k\delta\theta_{k'}e^{-iH_{J_1}t_1}\,|\varnothing\rangle_b \\
&= \langle\varnothing|_b\, e^{iH_{J_1}t_1}\delta\theta_k e^{-iH_{J_1}t_1}e^{iH_{J_1}t_1}\delta\theta_{k'}e^{-iH_{J_1}t_1}\,|\varnothing\rangle_b \\
&= \langle\varnothing|_b\,\delta\theta_{k,J_1}(t_1)\delta\theta_{k',J_1}(t_1)\,|\varnothing\rangle_b
\end{aligned} \tag{3.21}$$

where $\theta_{k,J_1}(t_1)$ is an operator written in the Heisenberg representation (the subscript J_1 tells us that the Hamiltonian used for the evolution is the one containing J_1). Quite nicely, if we write $\delta\theta$ in terms of creation/destruction operators, we just have to find out what is the time-evolution of these creation/destruction operators. We use the a basis in the computations, because it allows us to have the time evolution really easily. We get :

$$\delta\theta_{k,J_1}(t_1) = \frac{1}{\sqrt{2}}\frac{1}{\sqrt[4]{2J_1C(1-\cos(ka))}}(a_{k,J_1}(t_1) + a^\dagger_{-k,J_1}(t_1)) \tag{3.22}$$

The computation of the time evolution of the operators a and b is detailed in the appendix A.2. The result is that for an evolution with H_{J_1}, we have :

$$\begin{cases} a_k(t) = e^{-i\omega_{1,k}t}a_k \\ a^\dagger_k(t) = e^{i\omega_{1,k}t}a^\dagger_k \end{cases} \tag{3.23}$$

Equivalently, if we make evolve the b operators with H_{J_2}, we get :

$$\begin{cases} b_k(t) = e^{-i\omega_{2,k}t} b_k \\ b_k^\dagger(t) = e^{i\omega_{2,k}t} b_k^\dagger \end{cases} \tag{3.24}$$

We then obtain the expression of the operator $\delta\theta_{k,J_1}(t_1)$:

$$\delta\theta_{k,J_1}(t_1) = \frac{1}{\sqrt{2}} \frac{1}{\sqrt[4]{2J_1C(1-\cos(ka))}} (e^{-i\omega_{1,k}t_1} a_k + e^{i\omega_{1,k}t_1} a_{-k}^\dagger) \tag{3.25}$$

This time, we define : $B_{1,k} = \frac{1}{\sqrt{2}} \frac{1}{\sqrt[4]{2J_1C(1-\cos(ka))}}$. Now, what we have to do is look at how our operator expressed in the "a formalism" acts on the "vacuum" of the b formalism. We have to express all our a operators in terms of b operators with (3.16) to be able to compute this.

After some computations, which are in the appendix B.1 for the enthusiast reader, we get to our result :

$$\begin{aligned} \langle \Psi(t_1)| \, \delta\theta_k \delta\theta_{k'} \, |\Psi(t_1)\rangle = \frac{1}{2} \frac{1}{\sqrt{2J_1C(1-\cos(ka))}} \Bigg[& \frac{1}{2} \left(\sqrt{\frac{J_1}{J_2}} + \sqrt{\frac{J_2}{J_1}} \right) \\ & + \frac{1}{2} \left(\sqrt{\frac{J_1}{J_2}} - \sqrt{\frac{J_2}{J_1}} \right) \cos(2\omega_{1,k}t_1) \Bigg] \delta_{k,-k'} \end{aligned} \tag{3.26}$$

which can also be written as :

$$\langle \Psi(t_1)| \, \delta\theta_k \delta\theta_{k'} \, |\Psi(t_1)\rangle = \frac{1}{2} \frac{1}{\sqrt{2J_1C(1-\cos(ka))}} \left(\sqrt{\frac{J_1}{J_2}} \cos^2(\omega_{1,k}t_1) + \sqrt{\frac{J_2}{J_1}} \sin^2(\omega_{1,k}t_1) \right) \delta_{k,-k'} \tag{3.27}$$

From this, following the same steps as at $t_1 = 0$, we get :

$$\begin{aligned} \langle \Psi(t_1)| \, (\delta\theta_{j_1} - \delta\theta_{j_2})^2 \, |\Psi(t_1)\rangle = \frac{1}{N} \sum_k & \frac{1}{\sqrt{2J_1C}} \frac{1-\cos(k(r_{j_2}-r_{j_1}))}{\sqrt{1-\cos(ka)}} \\ & \cdot \left[\frac{1}{2} \left(\sqrt{\frac{J_1}{J_2}} + \sqrt{\frac{J_2}{J_1}} \right) + \frac{1}{2} \left(\sqrt{\frac{J_1}{J_2}} - \sqrt{\frac{J_2}{J_1}} \right) \cos(2\omega_{1,k}t_1) \right] \end{aligned} \tag{3.28}$$

As one can see in (3.27), if we put $t_1 = 0$, we recover the result of our previous computation which is a good sign that we are not mistaken.

Plots

Now, one can look at plotting these correlations to see what happens. To do this, we need to fix the parameters that we use. In Fig.3.1, we take $J_2 = 100, J_1 = 1, C = 1$ and we look at the difference of phases between neighbouring sites for different total number of sites.

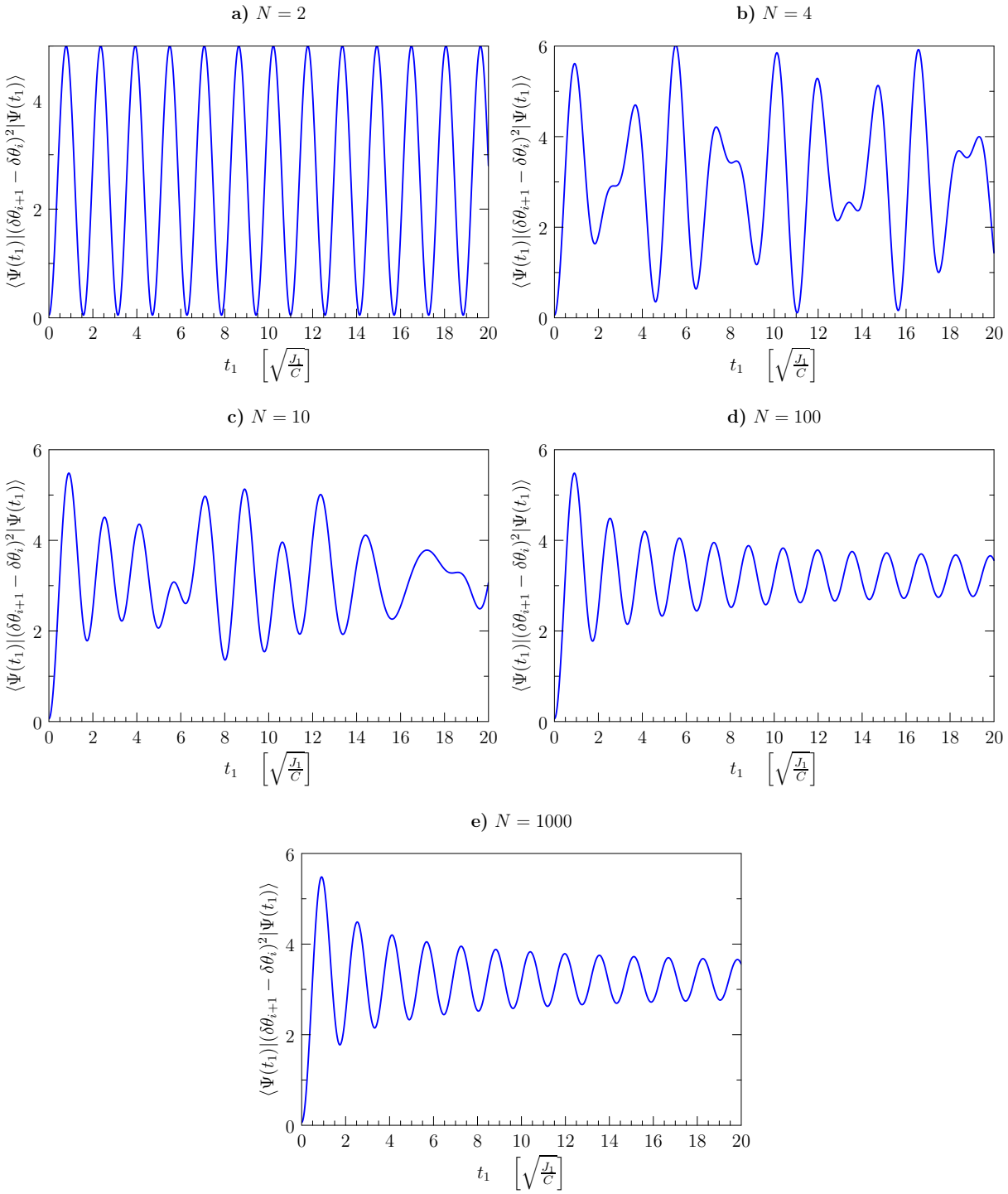

Figure 3.1 – Plots of $\langle\Psi(t_1)|\,(\delta\theta_{i+1} - \delta\theta_i)^2\,|\Psi(t_1)\rangle$ with $J_2 = 100, J_1 = 1, C = 1$ with different site numbers **a)** $N = 2$, **b)** $N = 4$, **c)** $N = 10$, **d)** $N = 100$, **e)** $N = 1000$

In (3.28), we see that we have a linear combination of functions with different periodicities, depending on the number of sites of the system. Therefore, the correlation are also a (quasi-)periodic function (the correlation could be not an exact periodic function because of the possible incommensurability of the frequences). For instance, with just 2 sites, there is only 1 mode which survives in the expression, therefore we end with a cosinus correlation function.
Some intermediate "damping" can be seen with 4 and 10 sites, where the oscillations are less "dampened". While with 100 and 1000 sites there is a damping of the oscillations which allows us to see better the average value, because of the number of different oscillations frequency. Furthermore, at this timescale, the "damping" is the same for these 2 number of sites. If we go on a longer timescale, while the 1000 sites are "dampened" more, we have reached the "maximal damping" for the 100 sites system.

Note that if we wait long enough, because our system is composed of a linear superposition of periodic functions, we will have some increase in oscillations at a certain timescale. This recrudescence period grows dramatically with the number of modes. Because of this, we focus on the short timescales, where we see the "damping" of the oscillations, without the recrudescence phenomenon.

For the rest of chapter 3, we fix the number of sites to 100 as a compromise between not seeing anything because of the oscillations and computation time.
Finally, we can see from Fig.3.1d), that the phase fluctuations difference oscillates around a value which is higher than the original one. This means that the phases of the different sites are less constrained to be close together.

As a small highlight, what is called here "damping" as nothing to do with a damping which could arise from a sort of friction because our system is completely isolated. It really comes just from the combination of several periodic functions with different frequencies.

Let us look now at the effects of the varying the coupling parameters J_1 and J_2. Fig.3.2 shows the plots of the correlations $(\delta\theta_i - \delta\theta_j)^2$.

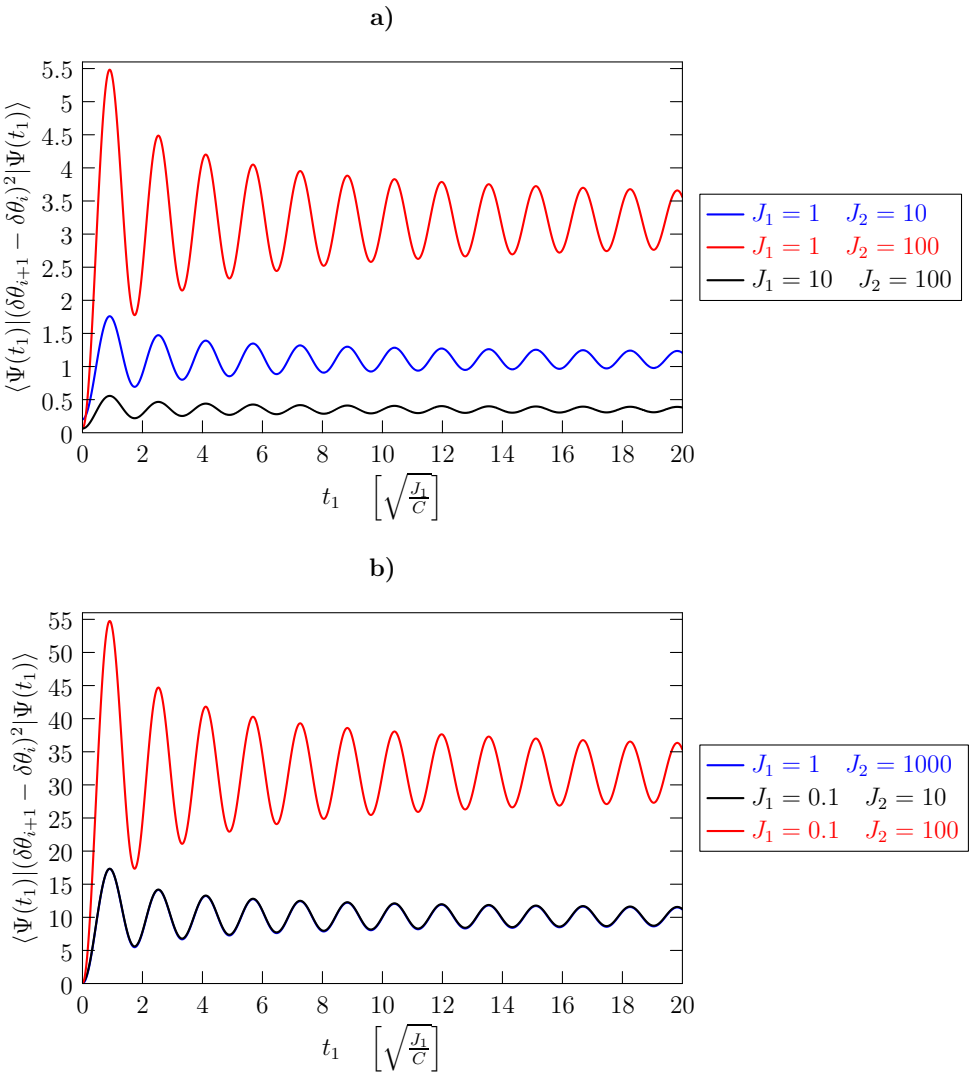

Figure 3.2 – Plots of $\langle\Psi(t_1)|\,(\delta\theta_{i+1} - \delta\theta_i)^2\,|\Psi(t_1)\rangle$ with $N = 100, C = 1$ with different pairs J_1, J_2. **a)** The pairs : $J_1 = 1$ and $J_2 = 10$, $J_1 = 1$ and $J_2 = 100$, $J_1 = 10$ and $J_2 = 100$. **b)** The pairs $J_1 = 1$ and $J_2 = 1000$, $J_1 = 0.1$ and $J_2 = 10$, $J_1 = 0.1$ and $J_2 = 100$. Here the first two pairs have the same values, therefore we see only one of them on the graph

There are two components in these plots, the oscillation frequency and the amplitude of the phase difference.
For the frequency of the oscillations, because of the choice of our time unit, we don't immediately see that the frequency of the oscillations depends of the choice of J_1. The larger J_1 is, the faster the oscillations occur, which comes from the fact that the oscillations terms in (3.28) are $\cos(2\omega_{1,k}t)$ with $\omega_{1,k} = \sqrt{\frac{2J_1}{C}(1-\cos(ka))}$ and therefore, the larger J_1 is, the faster the oscillations are.

On the amplitude of the phase difference, the common point in all these plots is that the

phase difference increases on the times shown (as mentioned before, the oscillatory nature of the correlation will lead to an increase of said oscillations which will then reach also low values but this is not the point). This corresponds intuitively very well with what we are trying to do, because we start from a system of sites which are strongly connected together, which favorize a small phase difference. And suddenly we loosen up the connection between the sites, thus favorizing a larger phase difference. The system follows this trend and we get larger $(\delta\theta_i - \delta\theta_j)^2$ values. Furthermore, the choice of J_2 fixes the starting point, and the choice of J_1 (given a certain J_2) determines the amplitude of the phase difference.

Indeed, the main difference between these plots is the amplitude of the phase difference. We see that the amplitude range can vary quite a lot for our different set of parameters. From below unity in the case of Fig.3.2e to around 50 in Fig.3.2f. Note that in this last case, the value of $(\delta\theta_i - \delta\theta_j)^2$ is definitely too large for our approximation of the cosine to still make sense and the results do not correspond anymore to a JJA model.

We also see that the sets in Fig.3.2b corresponding to the pairs $J_1 = 1, J_2 = 1000$ and $J_1 = 0.1, J_2 = 10$ have "almost" identical curves. We can look at the (3.28) to understand what we see. We see that the amplitude of the result is determined by 2 values : $\frac{1}{\sqrt{J_2}}$ and $\frac{\sqrt{J_2}}{J_1}$. In most of our cases, the first of these values is small compared to the second one which dominates, and this last is the same for the 2 sets mentioned before, which leads them to have "almost" identical results.

A small comment to be made is that in Fig.3.2, the starting points of the curve seem to be all the same, which would be in disagreement with (3.20). This is an effect of the scale of the figure. When we zoom enough, we indeed see that these plots have starting points which follow (3.20).

An other parameter that we can vary is the capacitance on each site C. We can see in Fig.3.3 the plots for two values of C : 0.1 and 1.

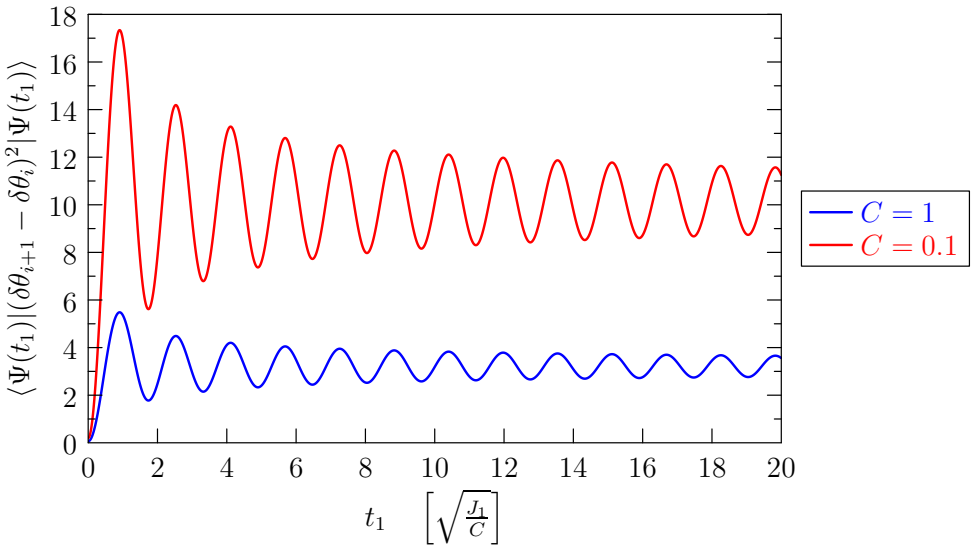

Figure 3.3 – Plots of $\langle\Psi(t_1)|\,(\delta\theta_{i+1} - \delta\theta_i)^2\,|\Psi(t_1)\rangle$ with $N = 100, J_1 = 1, J_2 = 100$ with different capacitances $C = 0.1, 1$

Again, the action of C impacts the frequency and the amplitude of the phase difference. If we look the expression of $\omega_{1,k}$ (A.5), we find the ratio $\frac{J_1}{C}$. Therefore, the effect of a change in C has the opposite effect of changing J_1 related to he frequency of the oscillation. And indeed this is what we see when we take into account the rescaling of the axes due to the change in C.

On the amplitude of the phase difference, the effect of C appears as factor $\frac{1}{\sqrt{C}}$. Therefore, the larger C is, the smaller the amplitude is. Intuitively, we are looking at systems which have different charging energies on the sites. When C is large enough, thinking in Bose-Hubbard model terms, it means that the contact interaction between bosons is small, which makes it easier to have several bosons on the same site, and this leads (compared to a system where C is smaller) to more tunneling between the sites, because there would be less repulsion of a particle already being on a given site when another one is coming. And therefore this leads to smaller phase difference.

One final variation that we can look at is what happens if instead of looking at the phase difference between neighbouring sites, we look at the phase difference between 10 sites or 50 sites. The phase difference for these 3 plots are shown in Fig.3.4 with the others parameters chosen as : $J_1 = 1, J_2 = 100, C = 1$.

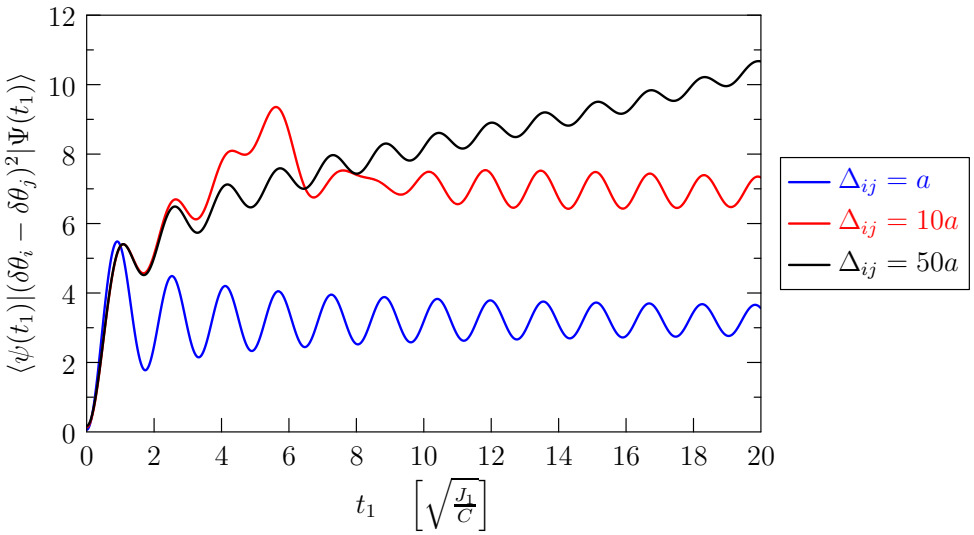

Figure 3.4 – Plots of $\langle\Psi(t_1)|\,(\delta\theta_i - \delta\theta_j)^2\,|\Psi(t_1)\rangle$ with $N = 100, J_1 = 1, J_2 = 100, C = 1$ with different distances $\Delta_{ij} = a, 10a, 50a$

What we can see here is that even if at first the behaviour is quite similar between the different distances, after this we get a regime where as we look at longer distances between the sites, the phase differences are larger as time advances. Intuitively, this seems reasonable, because the sites are still connected by a J_1 which is smaller than the J_2 and therefore there is a lesser constraint to have the same phase and this increases as we go further away. Note that if $J_1 = 0$, we would expect the correlation to be the same for all pair of sites, because having no link makes no difference in looking at neighbouring sites or opposite sites on our ring.

2.2.3 What happens at time t_2?

The next step is to look at what is the state of the system at t_2. We follow the same procedure as before to compute the observables. Here, we have to first write the $\delta\theta$ in terms of b to apply the evolution with H_{J_2}, then we have to write the b operators in terms of a, apply the evolution with H_{J_1} and rexpress the a operators in terms of the b ones to get the final result. For the very motivated reader, the calculations (which are really long) are in the appendix B.2.

Following are the correlations functions :

$$\begin{aligned}\langle\Psi(t_2)|\,\delta\theta_k\delta\theta_{k'}\,|\Psi(t_2)\rangle = \frac{\delta_{k,-k'}}{2\sqrt{2J_2C(1-\cos(ka))}}\Bigg[&\frac{1}{2}+\frac{1}{2}\cos(2\omega_{1,k}t_1)+\frac{1}{4}\left(\frac{J_1}{J_2}+\frac{J_2}{J_1}\right)\\&-\frac{1}{4}\cos(2\omega_{2,k}(t_2-t_1))\left(\frac{J_1}{J_2}-\frac{J_2}{J_1}\right)\\&-\frac{1}{4}\cos(2\omega_{1,k}t_1)\left(\frac{J_1}{J_2}+\frac{J_2}{J_1}\right)\\&+\frac{1}{4}\cos(2\omega_{2,k}(t_2-t_1))\cos(2\omega_{1,k}t_1)\left(\frac{J_1}{J_2}-\frac{J_2}{J_1}\right)\\&-\frac{1}{2}\sin(2\omega_{2,k}(t_2-t_1))\sin(2\omega_{1,k}t_1)\left(\sqrt{\frac{J_1}{J_2}}-\sqrt{\frac{J_2}{J_1}}\right)\Bigg]\end{aligned} \tag{3.29}$$

And, as previously, we have :

$$\langle\Psi(t_2)|\,(\delta\theta_{j_1}-\delta\theta_{j_2})^2\,|\Psi(t_2)\rangle = \frac{1}{N}\sum_k(2-2\cos(k(r_{j_2}-r_{j_1})))\,\langle\Psi(t_2)|\,\delta\theta_k\delta\theta_{-k}\,|\Psi(t_2)\rangle \tag{3.30}$$

Here again, if we put $t_2 - t_1 = 0$, the equations coincide with the previous ones. Also, if we put $J_2 = J_1$ we get the result of the time $t_1 = 0$. And finally if we choose $t_1 = 0$, we get the result when we did not evolve anything. All these correspondances are good sanity checks.

Plots

With these correlations, we have the same parameters that we can vary, and in addition we have also the time t_1 at which we stop the first time evolution. Just to remind ourselves of where we are in the protocol, we are now in the second blue part of Fig.2.4. We have let the system evolve for a time t_1 with a small coupling and now we restore the original coupling J_2 and we look at the time evolution of the system.

In Fig.3.5, we show several evolutions of $(\delta\theta_i - \delta\theta_j)^2$ for different pairs J_1, J_2, with $C = 1$ and $t_1 = 17\sqrt{\frac{J_1}{C}}$, for neighbouring sites and $N = 100$.

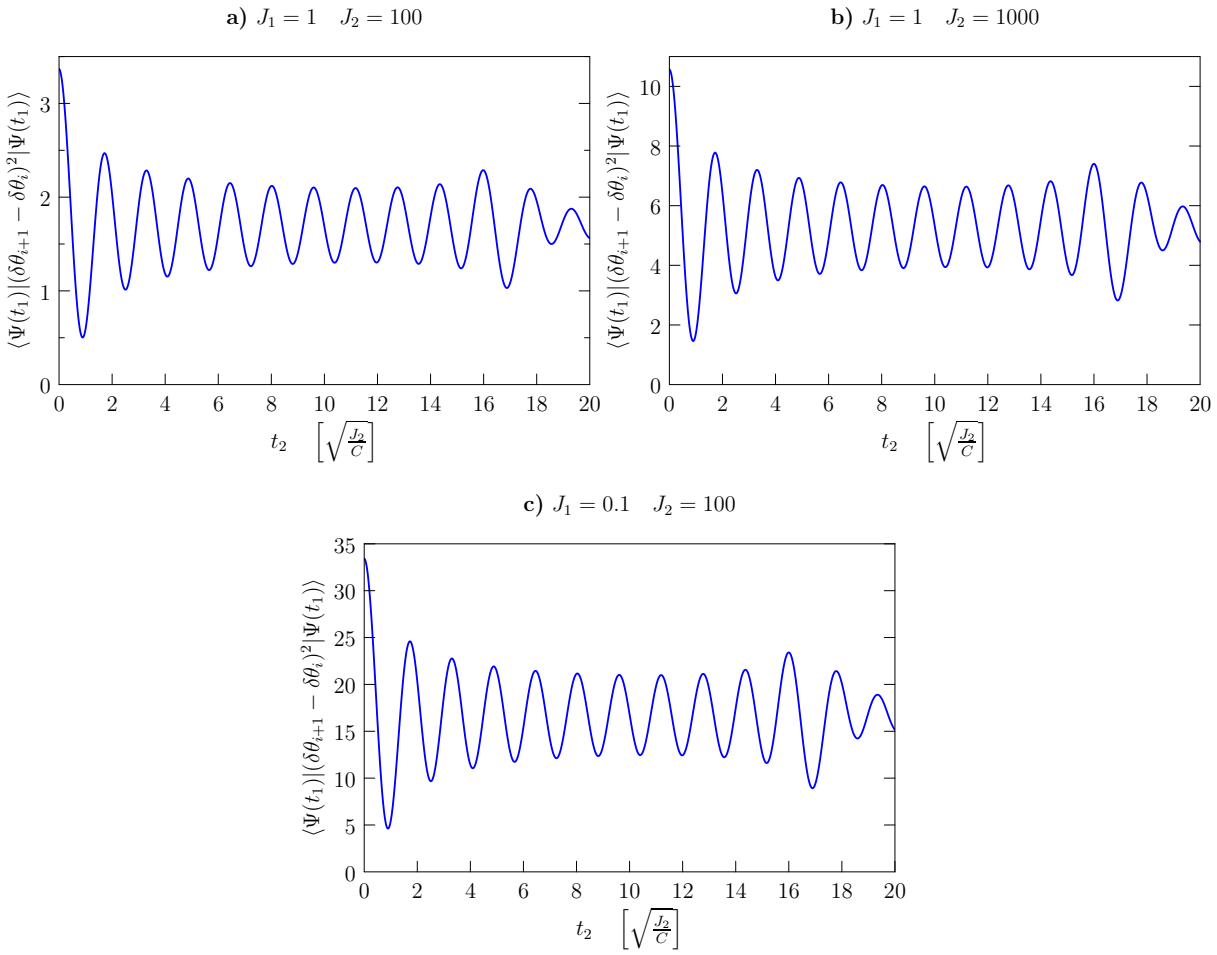

Figure 3.5 – Plots of $\langle\Psi(t_2)|\,(\delta\theta_{i+1} - \delta\theta_i)^2\,|\Psi(t_1)\rangle$ with $N = 100, C = 1$ with different pairs J_1, J_2. **a)** $J_1 = 1$, $J_2 = 100$. The value of the correlation before any quench was 0.06. **b)** $J_1 = 1$, $J_2 = 1000$. The value of the correlation before any quench was 0.02. **c)** $J_1 = 0.1$, $J_2 = 100$. The value of the correlation before any quench was 0.06.

The common element in all of these plots is, that while their amplitudes can be drastically different, all of them have a decrease in the phase difference with time. This corresponds well to what is intuitively expected when increasing J. Indeed, if looked from an quantum harmonic oscillator frame, here we would go from a relaxed potential to a strong potential. This leads to the fact that a same phase difference becomes more energy costly in the new Hamiltonian.

Because the system is isolated, it cannot dissipate the received energy and therefore the system cannot go back to its original state and cannot regain the original phase difference (as we can see with the caption of Fig.3.5). Instead, the system is excited in several modes. And here, the fact that we have 100 modes leads to the fact that getting back this same large phase difference is unlikely (at short times at least). For Fig3.5.c), we see that we are definitely in a regime where our approximation of the cosine is wrong.

In the following figure (Fig.3.6), we look at the effect of varying the time t_1. The other parameters are chosen as : $J_2 = 100, J_1 = 1, C = 1, N = 100$.

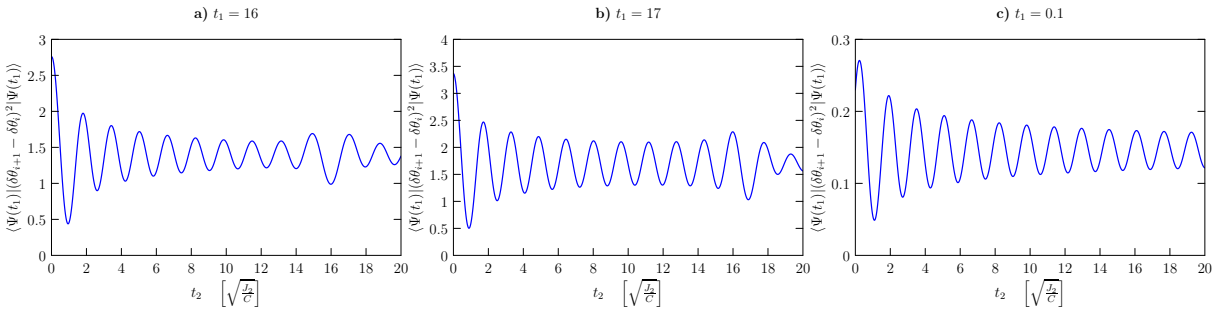

Figure 3.6 – Plots of $\langle\Psi(t_2)|\,(\delta\theta_{i+1} - \delta\theta_i)^2\,|\Psi(t_2)\rangle$ with $N = 100, J_1 = 1, J_2 = 100, C = 1$ with different times of quench t_1. **a)** $t_1 = 15$, **b)** $t_1 = 16$, **c)** $t_1 = 100$

We can extract from this figure that even when we are in the minima part of the oscillations for the phase difference in the J_1 evolution (Fig.3.6b), when we go to J_2, the system still want to lower the phase difference between neighbours. We also see that the average value is smaller than the one of Fig.3.6a, where we stopped the evolution with J_1 on a maxima of the oscillations. Therefore, even if the exact value of t_1 impacts the final state, it does it only quantitatively and not so dramatically. As long as we check to have a t_1 which leads to a value which is reasonably close to the average, we get qualitatively the same results and the choice t_1 does not matter in the physics which are happening.

On the other hand, looking at Fig.3.6.c), where we quenched back just after the first quench, we see that the system did not have enough time for the phases to explore what they could access and therefore the correlation is much closer to the original value. Hence there is a timescale in which the system does not have enough time to explore the possible values of phases and after an early second quench the system is back to a state close to the ground state.

Finally, we look at the variation of the phase difference if we look at different distances. We pick again $\Delta_{ij} = a, 10a$ or $50a$. The results are shown in Fig.3.7 :

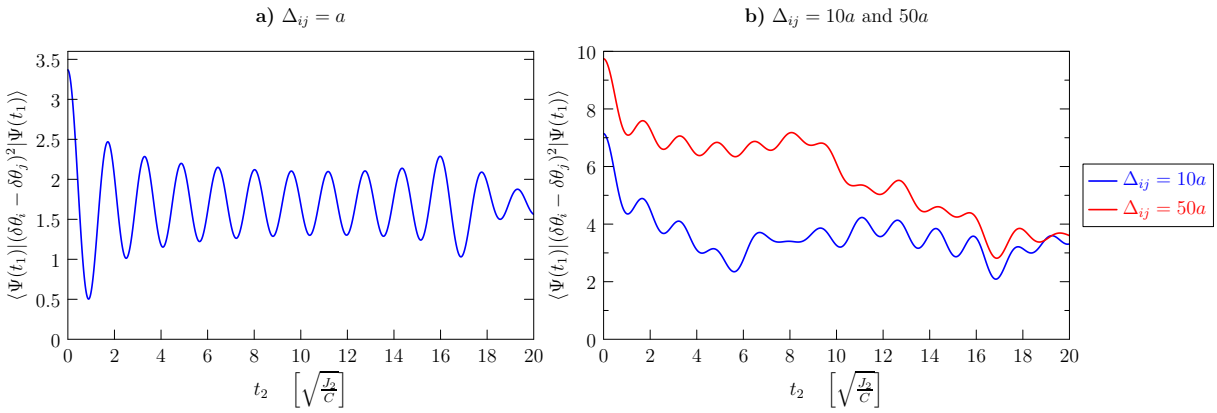

Figure 3.7 – Plots of $\langle\Psi(t_2)|\,(\delta\theta_i - \delta\theta_j)^2\,|\Psi(t_2)\rangle$ with $N = 100, J_1 = 1, J_2 = 100, C = 1$ for different distances Δ_{ij}.**a)** $\Delta_{ij} = a$ **b)** $\Delta_{ij} = 10a$ $\Delta_{ij} = 50a$

What we can say from Fig.3.7b, is that the phase coherence reinstalls itself (as much as it can) for all distances. Also the time needed to rephase depends on the distance that we look at which seems intuitive, because the information that all the sites are strongly coupled again needs some time to propagate along the system.

An important element of our system is that it conserves the energy. Indeed, there are no dissipation terms or couplings to an external bath in our system. This implies that our final state will never be the same as the initial state, because the system has been given energy in the quench procedure and by definition it cannot lose it. What the system does is that the energy oscillates between the phase difference term and the fluctuation of the number of particles term. Therefore, we get these oscillations in our observables.

One other element to look at is the validity of our solution for the Josephson Junction array model, because we assumed that the phase difference was small enough. Therefore, our solution is "dubious" when the phase fluctuations get large ($(\delta\theta_i - \delta\theta_j)^2 \approx 10$), because this leads to an higher energy state when we quench for the second time the system than what it should be if we had the cosine term (compare $\cos(\pi)$ with π^2). As a first approach to contain this in a reasonable way, we decided to add a term of mass for the phase fluctuations in the Hamiltonian as described in the appendix B.3. However, the results from this do not bring much new physics, therefore we do not present them here. Another way of avoiding the problem would be to take value of J_1 and J_2 which are closer to each other in order to inject less energy in the system and in this way keep the phase difference small enough.

We also looked at the effect of boundary conditions and solved the problem with box boundaries conditions, which lead to results which are qualitatively the same as in the problem in a ring. The only difference is that we have to use another transformation instead of the Fourier one to diagonalize our Hamiltonian (which is not so "nice" as the Fourier one to be written out). More details can be found in the appendix B.4. Here, we saw that qualitatively, the same conclusions could be extracted as in the periodic boundary case (even for 4 sites where the boundary effect is important). Therefore we do not show any plot of this case.

3 Summary and possibilities

In conclusion of this chapter, we were able to compute the correlations $\langle\Psi(t)|\,(\delta\theta_{j_1}-\delta\theta_{j_2})^2\,|\Psi(t)\rangle$ for all steps of our protocol (chapter 2, section 3) under the quadratic approximation of the JJA model. The result is a linear combination of oscillating modes.

We then looked at the effects of varying the different parameters of our system : the capacitance C which controls the amplitude of the correlations and the frequency of the oscillations, the pair of Josephson couplings J_2, J_1, which also controls the amplitude of the correlation with a certain ratio and depending at which time we look at the correlation, one of the coupling controls the frequency of the oscillations. The time of the second quench t_1 has a small effect on the averaged amplitude of the correlation at time t_2 because of the oscillatory behaviour of the correlations. There is also a timescale where if we requench the system, it has not enough time to lose the phase coherence and this is reflected on the final amplitude of the correlation. Finally the distance between sites where we looked at the correlation Δ_{j_1,j_2} showed us that there is some variation in the time needed to reach the average value.

Within the appendix B.3, we showed the calculations where adding a mass term to the phase fluctuations in order to stay in the regime where the quadratic approximation would still be correct and we looked at the case of box boundary conditions.

Further studies could look in more detail at the effect of the distance at which we look the correlation. This could lead to see a light-cone-like phenomenon as in [10] or [14]. Another possibility would be to try to implement a finite temperature in the system. Or one could also try to quench again and again the system with a given frequency and different behaviours could maybe emerge as a function of the frequency?

Chapter 4

Classical approach

Let us now tackle our system from a complete different point of view, where we take into account the temperature but drop out the quantum terms.

1 Idea

In this section, I justify a treatment of our system with a Langevin formalism. The first question to ask is : what is a Langevin formalism? To answer this, I start by explaining the Langevin equation.

1.1 Langevin equation

The origin of the Langevin equation is related to the Brownian motion. It is used to describe the motion of a "big" molecule in a fluid, and the catch of this problem is that this "big" molecule collides whith the "small" molecules which are contained in the fluid. For this, Langevin wrote the following equation of motion (4.1) :

$$m\frac{\mathrm{d}^2x}{\mathrm{d}t^2} + \eta\frac{\mathrm{d}x}{\mathrm{d}t} = F + \xi_x(\eta, T, t) \tag{4.1}$$

where m is the mass of the particle, x is its position, η is a friction parameter. F a force and ξ_x is a random thermal noise with a Gaussian probability distribution, and is chosen such that :

$$\overline{\xi_i(t)\xi_j(t')} = 2\eta k_b T\delta_{i,j}\delta(t-t') \tag{4.2}$$

where the subscripts $_{i,j}$ correspond to space indexes, k_b is the Boltzmann constant, T the temperature. The overline means an average over thermal noise and initial conditions. The δs ensure that the noise is spatially and temporally uncorrelated. This thermal noise is chosen such that in equilibrium the configurations are realized with a probability proportional to the Boltzmann weight $e^{-H/(k_bT)}$.

To apply this equation, we use the more "general" Langevin equation which is : [15]

$$\eta\frac{\mathrm{d}x}{\mathrm{d}t} = -\frac{\mathrm{d}H}{\mathrm{d}x} + F_{ext} + \xi_x(\eta, T, t) \tag{4.3}$$

Here, we have a direct link between the Hamiltonian and the Langevin equation and F_{ext} are external forces. We now have to look at our precise case.

1.2 Langevin equation in our case

The first question is why should we use the Langevin formalism in our system, what justifies it?

Well, if the temperature of the system is high enough and the quantum terms are small enough, a classical vision of the problem could be a good starting point. Furthermore, if we consider each site (with a large number of bosons on them in the lowest energy state) as a macroscopic particle with a given phase which interact with a thermal bath, there is an analogy with the original Langevin case with the "large molecule" colliding with the "small particles" of the fluid. One important difference with the case that we studied in chapter 3, is that here η (a phenomenological parameter) forces the system to reach a real thermal equilibrium by coupling it to the thermal bath and therefore we obtain a thermalization of our system.

We want to apply (4.3) to our system. At first, we see that we do not have any external forces. Therefore $F_{ext} = 0$.

Secondly, we assume that the the "capacitance" term in the Hamiltonian is negligible by respect to the temperature of system. This is a situation which is encountered in experimental realisations. (see section 5.3.3) We therefore do not have an inertial term in the Langevin equation and have only first time-derivatives.

Thirdly, in these approach we do not look at the fluctuations $\delta\theta_i$ of the phases, but we directly look at the phases θ_i.

Fourthly, because our phases are coupled together and we have several of them, we have a system of coupled equation of motions. For simplicity related to the comparison to an experiment which occurs in chapter 5, we choose to look at at system of 4 sites in a box (However, whenever possible we will give the expressions for a system with N sites).

Finally, we take box boundary conditions (and not periodic boundary conditions as in chapter 3), because it is this case that will be useful when comparing to an experiment (chapter 5). The difference is that here the first and last site have only one neighbour.

Our system of equations is then :

$$\begin{cases} \eta\frac{\mathrm{d}\theta_1}{\mathrm{d}t} = J\sin(\theta_2-\theta_1) + \xi_1(\eta,T,t) \\ \eta\frac{\mathrm{d}\theta_2}{\mathrm{d}t} = J(\sin(\theta_3-\theta_2) - \sin(\theta_2-\theta_1)) + \xi_2(\eta,T,t) \\ \eta\frac{\mathrm{d}\theta_3}{\mathrm{d}t} = J(\sin(\theta_4-\theta_3) - \sin(\theta_3-\theta_2)) + \xi_3(\eta,T,t) \\ \eta\frac{\mathrm{d}\theta_4}{\mathrm{d}t} = -J\sin(\theta_4-\theta_3) + \xi_4(\eta,T,t) \end{cases} \tag{4.4}$$

We now have to solve this system.

2 Technology : Analytics and numerics

There are two ways of tackling this problem. The first is to just head on and solve numerically this system. The other way would be to linearize the sines and solve the system analytically. What we do is solve the approximated system analytically and then use it to benchmark our numerical solution of the system.

2.1 Analytics

We linearize our system and get :

$$\begin{cases} \eta\frac{\mathrm{d}\theta_1}{\mathrm{d}t} = J(\theta_2-\theta_1)+\xi_1(\eta,T,t) \\ \eta\frac{\mathrm{d}\theta_2}{\mathrm{d}t} = J(\theta_3+\theta_1-2\theta_2)+\xi_2(\eta,T,t) \\ \eta\frac{\mathrm{d}\theta_3}{\mathrm{d}t} = J(\theta_4+\theta_2-2\theta_3)+\xi_3(\eta,T,t) \\ \eta\frac{\mathrm{d}\theta_4}{\mathrm{d}t} = -J(\theta_4-\theta_3)+\xi_4(\eta,T,t) \end{cases} \tag{4.5}$$

In order to diagonalize the system, we can write it in a matricial form :

$$\eta\frac{\mathrm{d}}{\mathrm{d}t}\vec{\theta} = J\underline{M}\vec{\theta}+\vec{\xi} \tag{4.6}$$

where $\underline{M}$ is :

$$\underline{M} = \begin{pmatrix} -1 & 1 & 0 & 0 \\ 1 & -2 & 1 & 0 \\ 0 & 1 & -2 & 1 \\ 0 & 0 & 1 & -1 \end{pmatrix} \tag{4.7}$$

which is of the more general form :

$$\underline{M}_{nxn} = \begin{pmatrix} -\alpha+b & c & 0 & 0 & \cdots & 0 & 0 \\ a & b & c & 0 & \cdots & 0 & 0 \\ 0 & a & b & c & \cdots & 0 & 0 \\ \cdots & \cdots & \cdots & \cdots & \cdots & \cdots & \cdots \\ 0 & 0 & 0 & 0 & \cdots & a & -\beta+b \end{pmatrix} \tag{4.8}$$

with $b=-2$, $\alpha=\beta=-1$ and $a=c=1$. This corresponds to the matrix studied in [16], where they find the eigenvalues (λ_k) and eigenvectors $u^{(k)}$ of these matrices, which are given by:

$$\lambda_k = b+2\sqrt{ac}\cos\left(\frac{(k-1)\pi}{N}\right) \qquad k\in[\![1,N]\!] \tag{4.9}$$

and

$$u_j^{(k)} = \cos\left(\frac{(k-1)\pi(2j-1)}{2N}\right) \qquad k\in[\![1,N]\!], j\in[\![1,N]\!] \tag{4.10}$$

We believe that there is a typo in the paper (we checked the eigenvectors by ourselves and the ones given by the paper weren't the good eigenvectors (some minus sign is missing/wrong in the paper)). By replacing all the parameters (except N), we get for the eigenvalues and eigenvectors :

$$\begin{cases} \lambda_k = 2(\cos\left(\frac{(k-1)\pi}{N}\right)-1) & k\in[\![1,N]\!] \\ u_j^{(k)} = \cos\left(\frac{(k-1)\pi(2j-1)}{2N}\right) & k\in[\![1,N]\!], j\in[\![1,N]\!] \end{cases} \tag{4.11}$$

After normalization of the eigenvectors (see Appendix C.1 for the details), we get the following transformations :

$$\begin{aligned}
\theta_k &= \frac{1}{\sqrt{N}} \sum_{j=1}^{N} \theta_j \qquad k = 1 \\
\theta_k &= \sqrt{\frac{2}{N}} \sum_{j=1}^{N} \cos\Big(\frac{(k-1)\pi(2j-1)}{2N}\Big)\theta_j \qquad k \neq 1 \\
\theta_j &= \frac{1}{\sqrt{N}}\theta_{k=1} + \sqrt{\frac{2}{N}} \sum_{k=2}^{N} \cos\Big(\frac{(k-1)\pi(2j-1)}{2N}\Big)\theta_k
\end{aligned} \tag{4.12}$$

And end up with a diagonal system (for 4 sites):

$$\eta \frac{\mathrm{d}}{\mathrm{d}t} \begin{pmatrix} \theta_{k=1} \\ \theta_{k=2} \\ \theta_{k=3} \\ \theta_{k=4} \end{pmatrix} = J \begin{pmatrix} \lambda_1 & 0 & 0 & 0 \\ 0 & \lambda_2 & 0 & 0 \\ 0 & 0 & \lambda_3 & 0 \\ 0 & 0 & 0 & \lambda_4 \end{pmatrix} \begin{pmatrix} \theta_{k=1} \\ \theta_{k=2} \\ \theta_{k=3} \\ \theta_{k=4} \end{pmatrix} + \begin{pmatrix} \xi_{k=1} \\ \xi_{k=2} \\ \xi_{k=3} \\ \xi_{k=4} \end{pmatrix} \tag{4.13}$$

We now have 4 decoupled Langevin equations which are the same in terms of form, whose solution is known and is :

$$\theta_k(t) = \theta_k(0) e^{\frac{J\lambda_k}{\eta}t} + \int_0^t \frac{1}{\eta} \xi_k(\eta, T, t') e^{\frac{J\lambda_{k'}}{\eta}(t-t')} \tag{4.14}$$

where $\theta_k(0)$ is the value of θ_k at time 0. An important thing to keep in mind, is that there is no exponential divergence in our solution, because all the eigenvalues are either 0 or negative. Our problem is now essentially solved, because thanks to the transformations (4.12) we have the exact time evolution of the phase on each site $\theta_i(t)$. We just need to compute our observables/correlation functions.

2.2 Protocols and observables

We follow the same kind of protocol that is described in section 2.3. But here we split it in two parts. The "rephasing" which corresponds to the times after t_1 in Fig.2.4, and the "dephasing" which corresponds to the times between t_0 and t_1 in Fig.2.4.

2.2.1 Rephasing

In the "rephasing", we assume that t_1 is large enough such that the starting state of system consists of random phases on each site. In the end we are interested in the correlation $\overline{(\theta_i - \theta_j)^2}$ as a function of time. In the same way as in chapter 3, we need the correlations $\overline{\theta_k(t)\theta_{k'}(t)}$ because we have to go to the diagonal expression of our system. We start by computing $\overline{\theta_k(t)\theta_{k'}(t)}$:

We start by plugging our results for $\theta_k(t)$ (4.14) in the correlation function. We get :

$$\overline{\theta_k(t)\theta_{k'}(t)} = \overline{\theta_k(0)\theta_{k'}(0)}(\cdots) + \int_0^t \overline{\theta_k(0)\xi_{k'}(t'')}(\cdots) + \int_0^t \overline{\xi_k(t')\theta_{k'}(0)}(\cdots) + \int_0^t \int_0^t \overline{\xi_k(t')\xi_{k'}(t'')}(\cdots) \tag{4.15}$$

We can simplify quite a lot this expression by looking at the correlations terms. Indeed, the correlations $\overline{\theta_k(0)\theta_{k'}(0)}$ are equal to 0 if $k \neq k'$ because we start with random phases : $\overline{\theta_i(0)\theta_j(0)}$ if $i \neq j$. The correlations $\overline{\theta_k(0)\xi_{k'}(t'')}$ are equal to 0 by definition. And finally, we have by using (4.2) and the transformations (4.12) that $\overline{\xi_k(t')\xi_{k'}(t'')} = 2\eta k_b T \delta_{k,k'}\delta(t'-t'')$.

This leads then to :

$$\begin{aligned}
\overline{\theta_k(t)\theta_{k'}(t)} &= \overline{\theta_k(0)^2} e^{\frac{2J\lambda_k}{\eta}t}\delta_{k,k'} + \frac{2k_bT}{\eta}\int_0^t\int_0^t e^{\frac{2J\lambda_k}{\eta}(t-t')}e^{\frac{2J\lambda_{k'}}{\eta}(t-t'')}\delta_{k,k'}\delta(t'-t'')\mathrm{d}t'\mathrm{d}t'' \\
&= \overline{\theta_k(0)^2} e^{\frac{2J\lambda_k}{\eta}t}\delta_{k,k'} + \frac{2k_bT}{\eta}e^{\frac{2J\lambda_k}{\eta}t}\delta_{k,k'}\int_0^t e^{\frac{-2J\lambda_k}{\eta}t'}\mathrm{d}t' \\
&= \overline{\theta_k(0)^2} e^{\frac{2J\lambda_k}{\eta}t}\delta_{k,k'} - \frac{k_bT}{J\lambda_k}\delta_{k,k'}\big(1-e^{\frac{2J\lambda_k}{\eta}t}\big)
\end{aligned} \tag{4.16}$$

There are some concerns which arise now. The first is what is the value of $\overline{\theta_k(0)^2}$. The second one which seems to be more dramatic is that one of our $\lambda_k = 0$ and we would have a special case to treat. We address them in this order.

The correlation $\overline{\theta_k(0)^2}$ is dependent on the initial condition of the system. In the case of the rephasing, we start from a random configuration. Therefore, we have a flat distribution of the θ between $-\pi$ and π. We then get :

$$\overline{\theta_k(0)^2} = \overline{\theta_i(0)^2} = \frac{1}{2\pi}\int_{-\pi}^{\pi}\theta_i^2\mathrm{d}\theta = \frac{\pi^2}{3} \tag{4.17}$$

where the first equality can be shown with the transformations (4.12).

The $\lambda_k = 0$ special case is resolved in quite a nice way, when we compute $\overline{(\theta_i-\theta_j)^2}$. Let us see it. Using the transformations (4.12), we get :

$$\begin{aligned}
(\theta_i(t)-\theta_j(t))^2 = \Big(&\frac{1}{\sqrt{N}}\theta_{k=1} + \sqrt{\frac{2}{N}}\sum_{k=2}^{N}\cos\Big(\frac{(k-1)\pi(2i-1)}{2N}\Big)\theta_k - \frac{1}{\sqrt{N}}\theta_{k=1} \\
&- \sqrt{\frac{2}{N}}\sum_{k=2}^{N}\cos\Big(\frac{(k-1)\pi(2j-1)}{2N}\Big)\theta_k\Big)(\cdots)_{k'}
\end{aligned} \tag{4.18}$$

We see, that the term where $k = 1$ which was the special one disappear from the correlations we are interested in. So it is not a problem. By looking at the eigenvector, this mode corresponds to the rotation of all the phases by the same amount. Therefore it is normal than when we look at the difference between phases this mode doesn't play any role.

We then get the expression (with some algebra in between) :

$$\begin{aligned}
\overline{(\theta_i(t)-\theta_j(t))^2} &= \frac{2}{N}\sum_{k=2}^{N}\Big(\cos\Big(\frac{(k-1)\pi(2i-1)}{2N}\Big) - \cos\Big(\frac{(k-1)\pi(2j-1)}{2N}\Big)\Big)^2\overline{\theta_k(t)\theta_k(t)} \\
&= \frac{2}{N}\sum_{k=2}^{N}\Big(\cos\Big(\frac{(k-1)\pi(2i-1)}{2N}\Big) - \cos\Big(\frac{(k-1)\pi(2j-1)}{2N}\Big)\Big)^2 \\
&\qquad\cdot\Big(\frac{\pi^2}{3}e^{\frac{2J\lambda_k}{\eta}t} - \frac{k_bT}{J\lambda_k}\big(1-e^{\frac{2J\lambda_k}{\eta}t}\big)\Big)
\end{aligned} \tag{4.19}$$

We can see that at large times, the exponentials tend to 0. Therefore the system loses all information about the initial configuration. And we get a equilibrium value :

$$\overline{(\theta_i(t)-\theta_j(t))^2} = -\frac{2k_bT}{NJ}\sum_{k=2}^{N}\Big(\cos\Big(\frac{(k-1)\pi(2i-1)}{2N}\Big)-\cos\Big(\frac{(k-1)\pi(2j-1)}{2N}\Big)\Big)^2\frac{1}{\lambda_k} \tag{4.20}$$

One element to notice is that this value can be greater than 2π because of the prefactor $\frac{T}{J}$ which appears in (4.20). This value beeing able to be greater than 2π comes from the fact that we keep track of how many turns of 2π our phases make. Because of the ratio $\frac{T}{J}$, we expect that for a given number of sites the equilibrium value is controlled by this ratio.

A further step that can be done is to look at the following quantity :

$$\overline{e^{i(\theta_i-\theta_j)}} = e^{-\frac{1}{2}\overline{(\theta_i-\theta_j)^2}} \tag{4.21}$$

This equality is valid for gaussian variables, which means that they follow a gaussian probability distribution. This is indeed the case for a quadratic hamiltonian as the one we are looking at. The catch will be the initial conditions of the phases. While this relation will be true at long times because of the effect of the noise which erase the specific of the starting conditions, at very short times, when we do this approximation, we have to be conscious that it might be an error because as our starting conditions for θ_i are not gaussian distributions.

In the limiting cases, we expect $\overline{e^{i(\theta_i-\theta_j)}}$ to be 1 if all the sites have the same phase, (because the difference of phases is 0), and 0 in the opposite limit. It is a better value to look at than $\overline{(\theta_i(t)-\theta_j(t))^2}$ because this one could technically go up to infinity where $\overline{e^{i(\theta_i-\theta_j)}}$ is bounded.

2.2.2 Dephasing

In the "dephasing", we look here at the case where the J_1 of Fig.2.4 has a specific value : $J_1 = 0$. Therefore, our system of Langevin equations (4.4) is already decoupled, and we obtain :

$$\theta_i(t) = \theta_i(0) + \frac{1}{\eta}\int_0^t \xi_i(\eta, T, t')\mathrm{d}t' \tag{4.22}$$

Then, we compute the correlation $\overline{(\theta_i(t)-\theta_j(t))^2}$ and after some algebra, we get :

$$\overline{(\theta_i(t)-\theta_j(t))^2} = \overline{(\theta_i(0)-\theta_j(0))^2} + \frac{4k_bT}{\eta}t \qquad i \neq j \tag{4.23}$$

This is an expected result, because we see that the more time we let evolve the system freely, the more the phases are decoupled between themselves. Here again, the initial condition $\overline{(\theta_i(0)-\theta_j(0))^2}$ do not matter in the final result which is the total uncorrelation between the phases. And in this case, we get that $\overline{e^{i(\theta_i-\theta_j)}}$ goes to 0.

2.3 Numerical solution

To go beyond the linearized case, we have to solve the problem numerically. We have the following Langevin equation to solve : (4.4) written in a general way, where we know that the terms with a θ_0 or θ_5 do not exist.

$$\eta \frac{\mathrm{d}\theta_i}{\mathrm{d}t} = J\big(\sin(\theta_{i+1} - \theta_i) - \sin(\theta_i - \theta_{i-1})\big) + \xi_i(\eta, T, t) \tag{4.24}$$

with the correlations for the thermal noise given by (4.2).

We include the thermal noise as :

$$\xi(t) = \sqrt{2\eta k_b T} z(t) \tag{4.25}$$

where $z(t)$ is a random number drawn from a Gaussian distribution with 0 mean and unit variance.

To solve this, we want to discretize the time and use the Euler method $\big(\frac{\mathrm{d}\theta_i}{\mathrm{d}t} = \frac{\theta_i(t+\epsilon)-\theta_i(t)}{\epsilon}\big)$, where ϵ is the Euler time step. The problem which arises, is that we need an Euler time step which is small enough to ensure that $\theta_i(t+\epsilon) - \theta_i(t)$ is small enough for different values of J. Therefore, we do a rescaling of our variables. We define :

$$\tilde{\theta}_i = \frac{\theta_i}{a} \qquad \tilde{t} = \frac{t}{b} \tag{4.26}$$

The rescaled variables have to satisfy the equations :

$$\frac{\tilde{\theta}_i\big(b(\tilde{t}+\tilde{\epsilon})\big) - \tilde{\theta}_i\big(b\tilde{t}\big)}{\tilde{\epsilon}} = \frac{b}{a}\frac{J}{\eta}\big(\sin(a(\tilde{\theta}_{i+1} - \tilde{\theta}_i)) - \sin(a(\tilde{\theta}_i - \tilde{\theta}_{i-1}))\big) + \frac{b}{a}\frac{\xi_i(\eta, T, b\tilde{t})}{\eta} \tag{4.27}$$

$$\overline{\xi_i(b\tilde{t})\xi_j(b\tilde{t'})} = \frac{2\eta k_b T}{b}\delta_{i,j}\delta(\tilde{t} - \tilde{t'}) \tag{4.28}$$

where $\tilde{\epsilon} = \frac{\epsilon}{b}$.
We implement the temperature with :

$$\xi(\tilde{t}) = \sqrt{\frac{2\eta k_b T}{b}} z(\tilde{t}) \tag{4.29}$$

And we choose b and a based on the parameters of the model. We have 2 equations :

$$\begin{aligned} A = 1 &= \frac{bJ}{a\eta} \\ B = 1 &= \frac{\sqrt{b 2\eta k_b T}}{a\eta} \end{aligned} \tag{4.30}$$

which is equivalent to :

$$\begin{aligned} a &= \frac{2k_b T}{J} \\ b &= \frac{2\eta k_b T}{J^2} \end{aligned} \tag{4.31}$$

Note that the constants A and B are arbitrarily chosen to be equal to one in our case, because it is simpler and works well numerically.

We now have the equation which relates the phases at time $t + \epsilon$ to the phases at time t :

$$\tilde{\theta}_i(\tilde{t} + \tilde{\epsilon}) = \tilde{\theta}_i(\tilde{t}) + \tilde{\epsilon}\big[\sin(a(\tilde{\theta}_{i+1}(\tilde{t}) - \tilde{\theta}_i(\tilde{t}))) - \sin(a(\tilde{\theta}_i(\tilde{t}) - \tilde{\theta}_{i-1}(\tilde{t})))\big] + \sqrt{\tilde{\epsilon}}z(\tilde{t}) \tag{4.32}$$

Here, a factor $\sqrt{\tilde{\epsilon}}$ arises form the discretization of the time in the correlation function (4.2). The only thing which has now to be fixed is the value of ϵ, which depend on the different parameters and by extension the one of $\tilde{\epsilon}$. Indeed, with a very large J, the evolution of the phases will be extremely fast and we need a smaller ϵ to be accurate than in the case where J is not that large. Because of the dependency of ϵ in the different parameters, it is more easy to fix a condition on $\tilde{\epsilon}$. We choose to keep $\tilde{\epsilon} < 0.01$ in order to ensure that the variation in $\tilde{\theta}$ and θ is small enough to justify the Euler method.

Once we have solved this equation numerically, it is almost over because having the values of $\theta_i(t)$, we can compute any observable that we want. To compute averages, we have to compute several realizations of $\theta_i(t)$ to take an average on the noise or/and initial conditions on the observable we want to study.

2.4 Numerics vs analytics : Benchmark

To benchmark our numerical method, we can use the same procedure but linearize all the sine and compare the results we get from it to the analytical results. We look at several linearized simulations compared to the analytical case to see if they match.

With the analytical prediction, what we get is the average $\overline{e^{i(\theta_i - \theta_j)}}$. Therefore, we have to do an average over our simulations. In this case, we do an average over 100 realizations. And because $e^{i(\theta_i - \theta_j)}$ is complex, we take only the real part of the average over 100 realizations.

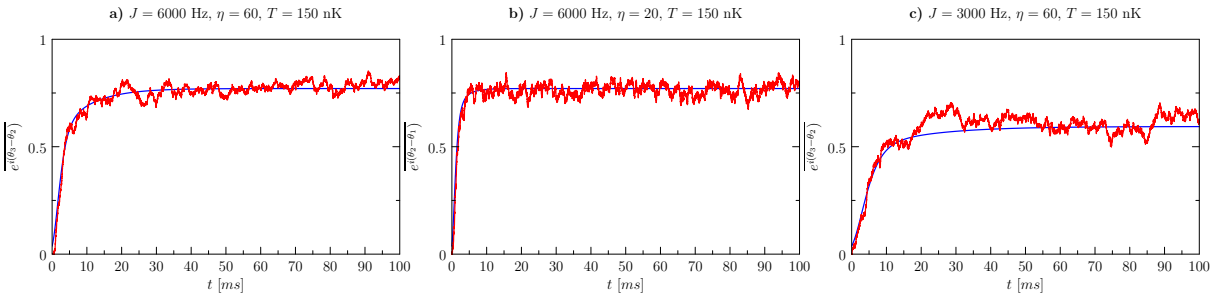

Figure 4.1 – Several comparisons of simulations linearized to analytical predictions of $\overline{e^{i(\theta_i - \theta_j)}}$, with different set of parameters.

Globally, we notice that there is a really good agreement between the simulations and the analytical prediction. The small differences which can be seen are caused by the fact that we did not average over an infinite amount of simulations and therefore it can happen that we have bad luck with the thermal noise. Our benchmark is now completed and it is reasonable to trust the results coming form the same program where we don't linearize the sines.

We now have all the tools to look at a concrete implementation of this model to an actual experiment of quenches in dipolar cold atoms.[12]

Chapter 5

Classical approach : Comparison with an experiment

1 Experiment of Ferlaino's group

The experiment which we are interested in has been realized in Ferlaino's group at the University of Innsbruck, where they study the evolution of the phase coherence of supersolid phases in an ultracold atom gas when subject to quenches.

The first question to answer is why should a Josephson Junction array model correspond to the experiment in question. The answer (yes) to this question is contained in the definition of the supersolid phase.

1.1 Supersolid

A supersolid phase is a phase that has properties of both the superfluid order and the solid order. More specifically, as in a solid, a supersolid breaks the translation symmetry, it has a density modulation in space. On the other hand, as in a superfluid, the phase symmetry is broken and there is a global phase coherence in all the supersolid. A supersolid posess these two characteristics simultaneously.

In the Ferlaino's experiment, they put a gas of dipolar atoms in a cigar-shaped trap. A sketch of this can be seen in Fig.5.1a. By playing with the scattering length and the atom number, they can achieve several phases shown in the phase diagram (Fig.5.1b), namely a Bose-Einstein condensate (BEC), the supersolid phase (SSP) and an isolated droplet phase (ID). Starting from the BEC, where the gas forms only one large droplet (insert in Fig.5.1b). When decreasing the scattering length, the system self-organizes itself in a serie of droplets which are connected between them. This allows an exchange of particles between the different droplets and is the SSP. Finally, by further decreasing the scattering length, one cuts the links between the droplets and ends in the ID phase.[17],[12]

A Josephson Junction array can describe well these last two phases. Indeed, for the ID, it would correspond to a JJA where there is no tunneling between the different sites, while in the SSP, we are in the situation where there is exchange of particles between the different sites and this can be described by JJA. The only limitation is that we have to be able to define the

different sites to be able to tell what is the site and what is the junction. Therefore there is a limit when going to the BEC phase where the JJA model is not anymore a good model.

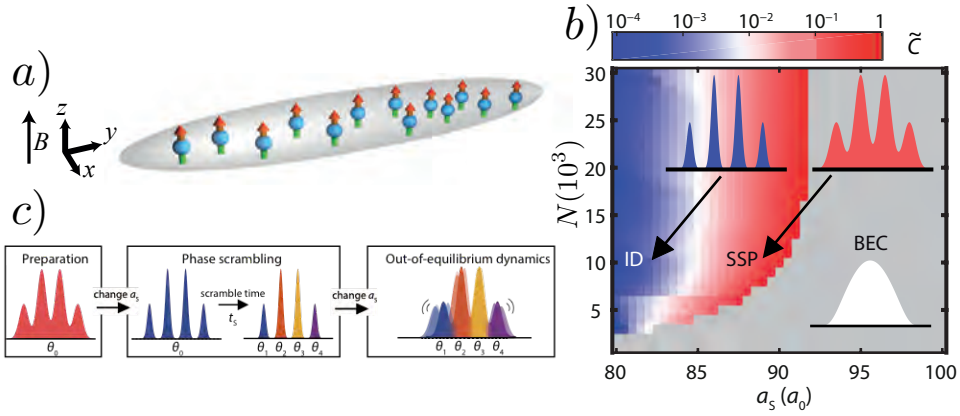

Figure 5.1 – **a)** A sketch of the gas trapped in a cigar-shaped potential **b)** Phase diagram of the cigar-shape trapped gas. The inserts show the density profiles of the different phases. **c)** Protocol of scrambling and rephasing [17],[12]

In their experiment, Ferlaino's group follows the protocol described in [12] by changing the scattering length as depicted in Fig.5.1c. First they go from the SSP phase to the ID phase, which corresponds to cutting the link between the different droplets. Then they let the droplets evolve independently for 20 ms. After this scrambling, they set again the scattering at the original value in the SSP phase and look at the evolution of the phase coherence in the system (rephasing).

1.2 Observable

A crucial point is what do they measure in the experiment. Of course it would be absolutely ideal to be able to get the phase difference between each droplet, but it is not possible. From their interference measurement, they get a quantity which is related to the phase differences, called phasor.[12] It is then possible to relate the phase of the phasor to the phase differences predicted by our JJA model by :

$$\Phi = \arg\left(\sum_{j=1}^{3} e^{i(\theta_{j+1}-\theta_j)}\right) \tag{5.1}$$

An observation is that some of the phase differences fluctuations are smoothened by the definition of Φ, meaning that Φ fluctuates less than $\theta_i - \theta_j$ because it is an average over several phase differences.

From this Φ, they compute the circular variance, which is defined as :

$$\Delta\Phi = 1 - \frac{1}{q}\sqrt{\left(\sum_{i=1}^{q}\cos(\Phi_i)\right)^2 + \left(\sum_{i=1}^{q}\sin(\Phi_i)\right)^2} \tag{5.2}$$

where q is the number of realizations.

To try to understand a bit what happens with this $\Delta\Phi$ and Φ, let us look at the extremal cases. First, let us consider that all the droplets have the same phases. We then get that $\Phi = 0$ and therefore $\Delta\Phi = 1 - \frac{1}{q}\sqrt{q^2} = 0$. On the opposite limit, if every difference of phase is completely random, the Φ will also be random and in the expression of $\Delta\Phi$, only the diagonal terms will survive, leading to $\Delta\Phi = 1 - \frac{1}{\sqrt{q}}$. If we look at our procedure of rephasing, where we start from random phases and let the system evolve with a given J, if J is large enough, $\Delta\Phi$ should start at $1 - \frac{1}{\sqrt{q}}$ and decrease.

In their experiment, they take between 60 and 100 Φ to compute $\Delta\Phi$. To match this, we take in all our simulations 100 realizations and compute $\Delta\Phi$ with those 100 simulations. Therefore, the maximal equilibrium value of $\Delta\Phi$ that we will get is 0.9. As a final step, we will average $\Delta\Phi$ over 4 simulations to average a bit more the thermal noise.

2 Effects of the different parameters

In this part, we look at what is the impact of the different parameters of system in our JJA model when looking at $\Delta\Phi$. We look at the coupling between the sites with J, the effect of the friction η, the effect of the temperature T and what happens if we vary the number of sites. We take as "default" values the ones that correspond well to the experiment : $J = 6000$ Hz, $\eta = 60$, $T = 150$nK, and 4 sites.

2.1 Effects of change of J

As a first parameter we look at, let us vary J and do our rephasing procedure. Starting from a random phase configuration and letting the system evolve with a given J. The temperature that we take is of 150 nK. The η that we take is of 60. Several rephasing curves can be seen on Fig.5.2.

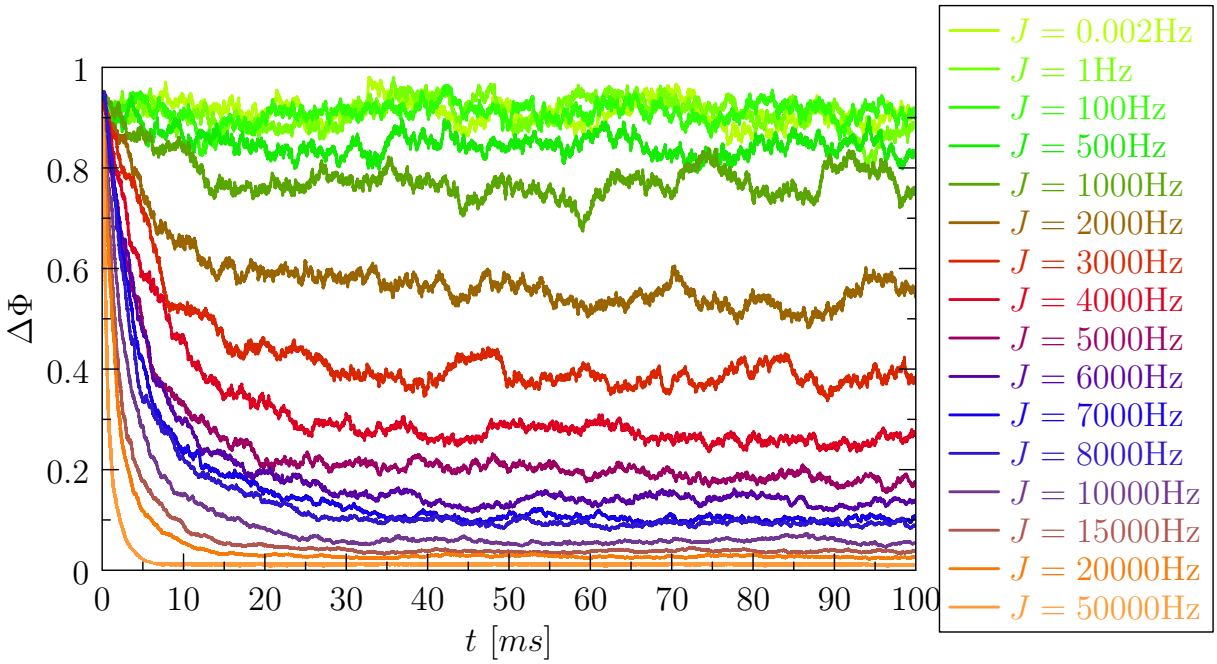

Figure 5.2 – Comparison between different J of the rephasing procedure, looking at $\Delta\Phi$ with a fixed value of $\eta = 60$ and $T = 150$nK.

What we notice is that we scan all the space of $\Delta\Phi$ with our range of J. This is completely reasonable, because the equilibrium is determined as metioned after (4.20) by the ratio between T and J. There is a competition between the J which wants to lock all the phases at the same value and the temperature which wants to have random phases on each site. Our temperature corresponds to 3000 Hz. Therefore it is expected that when the J is small enough, absolutely no rephasing can be seen. The opposite is also true, when J is much larger than the temperature, the phase are very well locked and further increasing J does not change significantly the large time behaviour of $\Delta\Phi$. Another way of phrasing it is that then one of the two parameters dominates, increasing the dominating parameter does not affects much the equilibrium state of the system.

An other effet of the parameter J is that it also controls the time needed to reach the equilibrium. The larger J is the faster the system reaches it's equilibrium state. This goes along the same direction as the linearized version in (4.19), where in the exponetial which contain the time evolution there is a J and the fact that for large J the needed value of ϵ in the numerical solution is way smaller than for small J.

One important thing to note about (4.19), is that its validity is only when the difference between 2 phases is small. Therefore it is valid only for large J close to the equilibrium state. The fact that the general behaviour coming from this equations is also true is not surprising but was not a certitude.

2.2 Effects of change of η

The other main parameter that we can vary is η. In Fig.5.3 there are plots of $\Delta\Phi$ for several ηs, with $J = 6000\,\text{Hz}$ and $T = 150\text{nK}$.

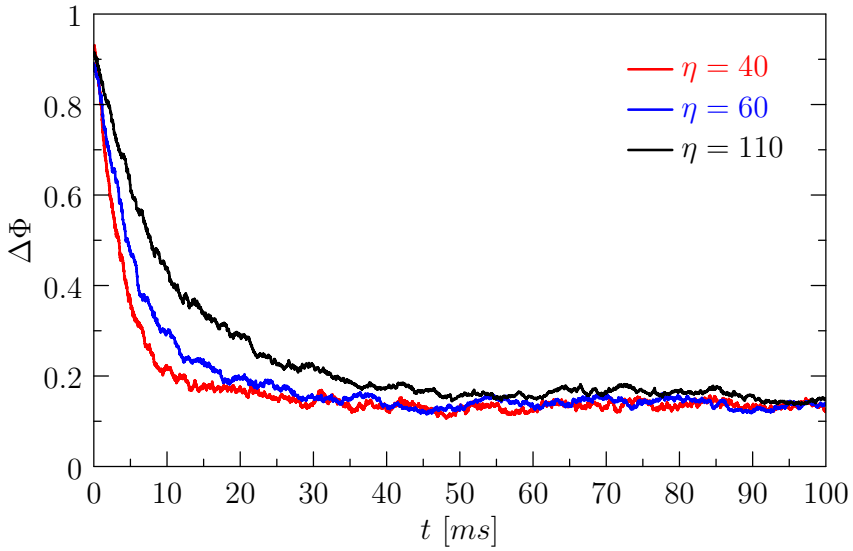

Figure 5.3 – Comparison between different η of the rephasing procedure, looking at $\Delta\Phi$ with $J = 6000$ Hz and $T = 150$ nK.

What we observe is that η controls only the time scale on which the evolution occurs, which was already indicated in (4.19) where η apperared only in the exponentials containg the time. The larger η is, the larger is the time needed to achieve the equilibrium state. On the opposite side, the smaller the η is, the faster the system reaches its equilibrium.

Another comment about η is that η is a phenomenological parameter which describes the coupling of the system to the thermal bath, but also to all the other degrees of freedom that the system might have which are not included in the rest of our Langevin treatment.

2.3 Effects of change in temperature

We can also vary the temperature of the system. To look at its effects, we considered several temperatures (10nK, 150nK and 1000nK). We kept for these 3 cases $J = 6000$ Hz and $\eta = 60$. The plots are shown in Fig.5.4.

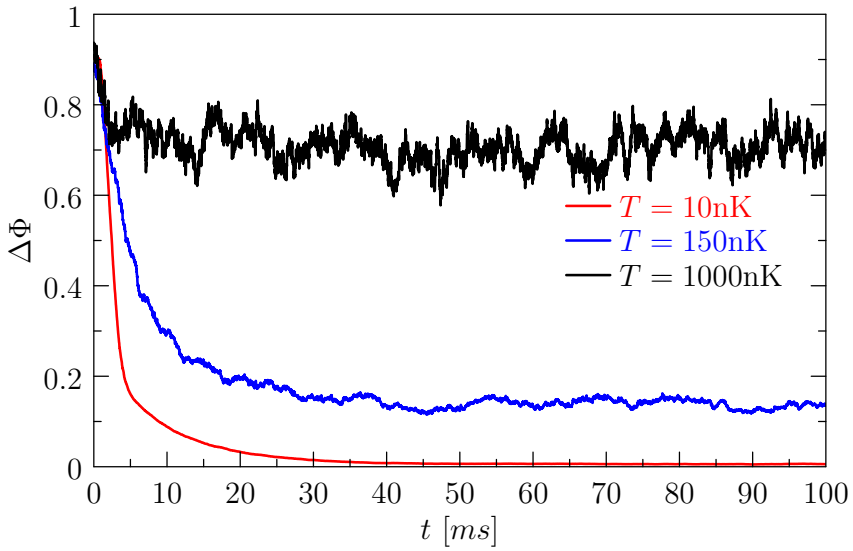

Figure 5.4 – Comparison between different temperatures of the rephasing procedure, looking at $\Delta\Phi$ with $J = 6000$ Hz and $\eta = 60$.

As expected, because of the competition between J and T, the first thing that we notice is that the temperature influences the equilibrium value of $\Delta\Phi$. The stronger T is, the more the phase fluctuates and the closer the $\Delta\Phi$ is to 0.9. We also see that the temperature does not seem to impact the speed at which the system reaches the equilibrium value, as was strongly suggested by (4.19), where the temperature is not involved in the time-evolution terms.

2.4 Effects of change of the number of droplets

One other parameter that we can vary in our system is the number of droplets that compone it. In this case, the only difference is that our Langevin equation system changes in an appropriate way as does the definition of Φ. In Fig.5.5, we see the difference between $2, 3, 4$ and 5 sites.

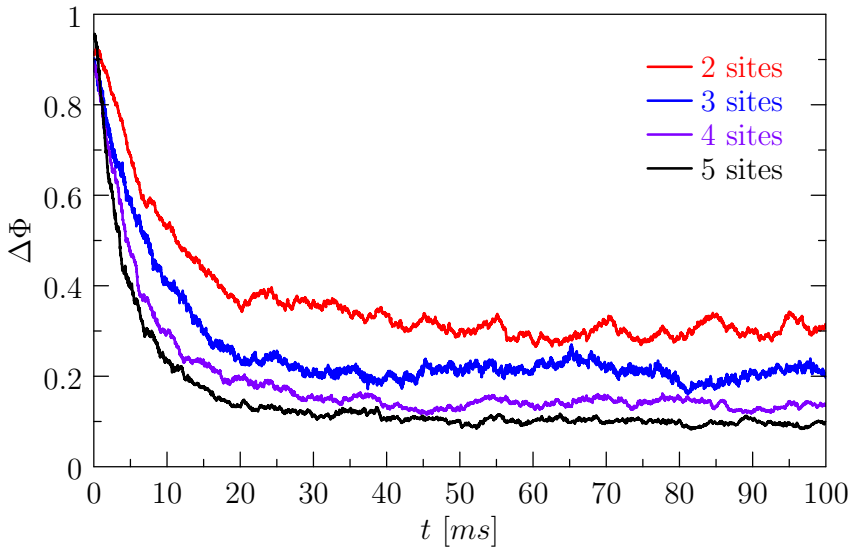

Figure 5.5 – Comparison between different site numbers of the rephasing procedure, looking at $\Delta\Phi$ with $J = 6000$ Hz, $\eta = 60$ and T=150 nK.

What we observe is that the more sites the system has, the smaller the equilibrium value of $\Delta\Phi$ is and there seems to be no great influence of the number of sites to the timescale of the evolution. This goes well with the analytical solution of the linearized case where we had a factor $\frac{1}{N}$ in the expression of $\overline{(\theta_i(t) - \theta_j(t))^2}$.

A further element to notice is that by the definition of Φ, we get a smaller Φ as the number of sites increase because for 2 sites Φ is the difference of phases between the two sites so we have all the fluctuations of $\theta_i - \theta_j$, while with more sites we start to average these fluctuations, and therefore the value of $\Delta\Phi$ decreases even more.

With this, we ended our tour of the effects of the different parameters on the model and it is now time for a direct comparison to an experiment.

3 Application of the model to Ferlaino's experiment

To applicate the model to the experiment and check if it is indeed a good model, we need to fix the different parameters in the model. Fortunately, with several measures we can indeed fix all the parameters. First of all, the temperature of the experiment can be measured ot was found to be varying a bit around 150nK. We then take $T = 150$nK. We still need to fix J and η.

3.1 Fixing the parameters J and η

To fix J, we use the fact that the equilibrium value of $\Delta\Phi$ does not depend on the parameter η but only on J and T. We then compare the equilibrium value of the predicted $\Delta\Phi$ with the experimental long time value of $\Delta\Phi$. We find that a good agreement is obtained with $J = 6000$ Hz. We get $\Delta\Phi_{JJA} \approx 0.138$ and $\Delta\Phi_{exp} \approx 0.142$.

To find η, we use the dephasing measurement. In this, we try to follow closely the evolution in J as in the experiment. We do a linear ramp of 20 ms of J from 6000 Hz to 0.002 Hz. This latter value comes from an estimation of the tunneling between different sites in the ground state of the system by using the extended Gross-Pitaevskii equation.[17] As shown in Fig.5.6, the value of $\eta = 60$ matches very well the experimental data, and we choose the $\eta = 60$ for the following analysis.

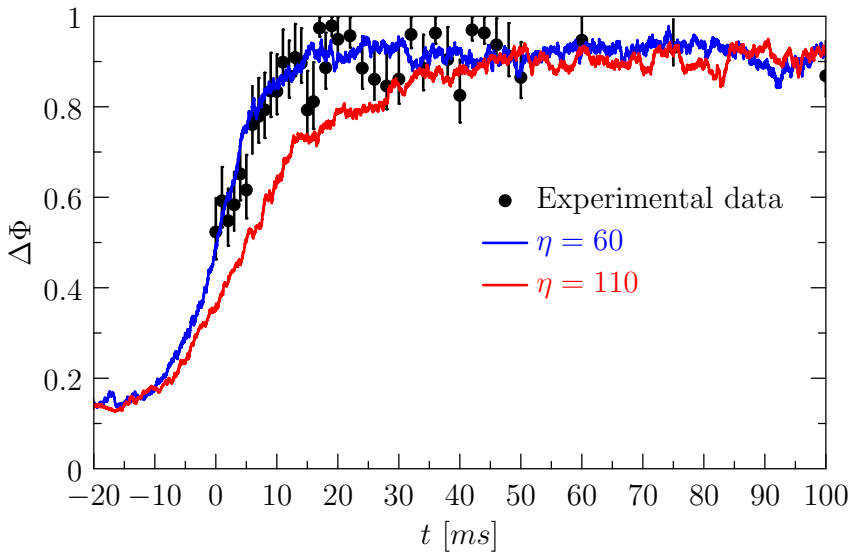

Figure 5.6 – Comparison between two values of η in the JJA model and the experimental data for the dephasing procedure.

3.2 Comparing the rephasing

With all the parameters of our model fixed, we can finally look at how well does our model reproduce the rephasing curve, where we change instantly from $J = 0.002$ Hz to $J = 6000$ Hz. In Fig.5.7, we see the experimental data of the rephasing and also the predictions for 2 values of η: 60 and 110.

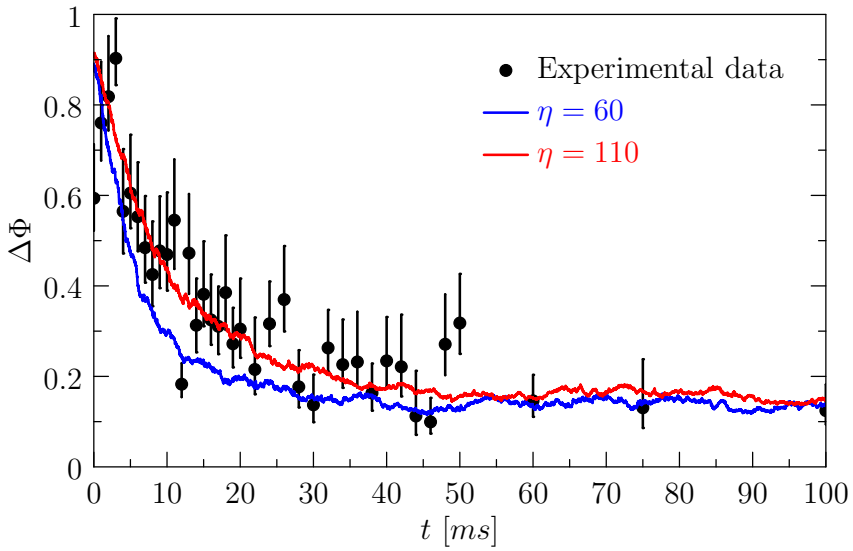

Figure 5.7 – Comparison between two values of η in the JJA model and the experimental data for the dephasing procedure.

As we can see, the curve with $\eta = 60$ qualitatively predicts well the rephasing curve. The plateau value at large times as well as the timescale to reach the plateau are consistent with the experiment. However, at small times, the JJA curve is systematically below the experimental data. Instead, if we take $\eta = 110$, the JJA curve fits the rephasing curve well, but the related dephasing curve (Fig.5.6) does not agree with the experimental data. This suggests that there are phenomena which occurs in the rephasing and not in the dephasing (hence the different value of η to fit these 2 cases). One possibility to explain this could be that because the droplets are self-formed, they have also the possibility to spatially oscillate which would lead to the Josephson coupling having the possibility of varying as function of the droplet's positions and this is definetely not contained in the JJA model that we used.[12]

3.3 Discussion about C-term

One element which there is still to discuss is why shoud we neglect the C-term in the Langevin equation in this case. To answer this, we estimated the value of the energy related to the C-term by using a variational approach to find the ground state of the supersolid.[18].

The ground state ansatz is taken as a droplet array in the z-direction with :

$$\Psi_{DA}(\mathbf{x}) = \sqrt{\frac{N_D}{\pi^{3/2} l^2 l_z}} e^{-(\mu x^2 + y^2/\mu)/2l^2} e^{-z^2/2l_z^2} \tag{5.3}$$

where N_D is the number of atoms in a droplet, l and μ describe the mean width and anisotropy of the droplets in the transversal directions, l_z sets the size of the droplets along the array. Each droplet is separated by a distance L, which is large enough to have well separated droplets : $L \gg l_z$ which fixes the density : $N_D = nL$.

The energy per particle is given by :

$$E_{DA} = E_\perp + \frac{\hbar^2}{4ml_z^2} + \frac{\hbar^2 nL}{\sqrt{2\pi}ml^2 l_z}\left(a_s + a_{dd}\frac{f(\kappa)+1-\mu}{1+\mu}\right) + g_{QF}\left(\frac{2nL}{5\sqrt{\pi}l_z}\right)^{3/2} + \frac{3na_{dd}\hbar^2}{mL^2}\zeta(3) \quad (5.4)$$

where $E_\perp$ is the transversal energy associated to the trap, m is the mass of the atoms in the system, a_s is the scattering length, $a_{dd} = \frac{m\mu_o\mu_m^2}{12\pi\hbar^2}$ is the dipole length where μ_o is the vacuum permeability and μ_m is the magnetic moment of the atoms of the system, $f(\kappa) = \frac{1+2\kappa^2-3\kappa^2\text{atanh}(\sqrt{1-\kappa^2})/\sqrt{1-\kappa^2}}{1-\kappa^2}$, $\kappa = \mu^{1/4}l/l_z$, $g_{QF} = \frac{256\hbar^2}{15m(\sigma_y\sigma_x)^{3/2}}a_s^{5/2}(1+\frac{3}{2}(\frac{a_{dd}}{a_s})^2)$ is a coefficient related to quantum fluctuations and ζ is the Riemann function. We also use $\sigma_x = l/\sqrt{\mu}, \sigma_y = l\sqrt{\mu}, \sigma_z = l_z$. We take as numerical values typical values of the ground state calculations : $a_s = 5$ nm, $\sigma_z = 0.5$ μm, $\sigma_x = 0.8$ μm and $\sigma_y = 2$ μm. We also have that because the atoms that are used are of Dysprosium, they have a magnetic moment of $9.9\mu_B$ (Bohr magneton) and a mass of $2.7 \cdot 10^{-25}$ kg.

The second term of 5.4 corresponds to the kinetic energy of the particle in the system. The third term describes the intra-droplet interactions, which are splitted in contact interactions and dipole-dipole interactions. The fourth term is a quantum fluctuation correction and the last term is the inter-droplet (long range) interaction coming from the dipoles.

To recover the capacitance term, we look at how much energy it costs to take one particle from a droplet and put it on another one. In this way, we do not have to pay for the chemical potential (i.e. the energy cost to bring the particle in the system), but we see really the charging cost. The relevant terms in (5.4) are the three last terms.

For the intra-droplet term, the energy goes with N^2, with N being the number of atoms on the droplet and n large enough. We have then to look at $(N+1)^2 + (N-1)^2 - N^2 = 2$. We then have that with (5.4) for the contact part :

$$\Delta E_{contact} = \frac{2\hbar^2 a_s}{\sqrt{2\pi}m\sigma_x\sigma_y\sigma_z} = 0.31\text{Hz} \quad (5.5)$$

and for the dipole-dipole part :

$$\Delta E_{dd} = \frac{2\hbar^2}{\sqrt{2\pi}m\sigma_x\sigma_y\sigma_z}a_{dd}\frac{f(\kappa)+1-\mu}{1+\mu} = -0.30\text{Hz} \quad (5.6)$$

For the quantum fluctuation term, we have that the energy goes with $N^{5/2}$. Because, we consider that $N \gg 1$, we get that : $(N+1)^{5/2} + (N-1)^{5/2} - 2N^{5/2} \approx \frac{15}{4}\sqrt{N}$. We take $N = 4000$ for the computation and we get :

$$\Delta E_{QF} = \left(\frac{2}{5\sqrt{\pi}\sigma_z}\right)^{3/2} g_{QF}\frac{15}{4}\sqrt{N} \approx 0.25Hz \quad (5.7)$$

For the inter-droplet term, we assume that we can consider the two droplets as two giant dipoles who are at distance L. Here, the energy goes as $N_1 * N_2$. Therefore we look at : $(N+1)(N-1) - N^2 = -1$. With the last term in (5.4), we get that :

$$\Delta E_{interdroplet} = -\frac{3a_{dd}\hbar^2\zeta(3)}{mL^3} \approx -0.012\text{Hz} \tag{5.8}$$

The total energy change is the sum of these 4 terms, which is of the order of the Hz, which is completely negligible in front of the temperature (3000 Hz). Therefore it is justified to neglect the capacitance term in the Langevin equation.

Chapter 6

Conclusion and Perspectives

We have studied a 1D Josephson Junction array model under a "double-quench" protocol in two very distinct limits. We started with the system in the ground-state of a given JJA hamiltonian, then decreased the Josephson coupling and let the system evolve in this "dephasing" regime and finally restored the original value of the Josephson coupling and look at what happened.

The first limit was at $T = 0$K and periodic boundary conditions, we used a quadratic approximation on the Hamiltonian in order to treat it analytically. We then explored the different effects of the parameters ranging from the coupling constants to the distance at which we looked at the phase correlations. Because of the finite number of sites that we looked at, all our results where linear combinations of periodic functions, which then had a recrudescence of values which are far from the average ones. The main conclusions out of this exploration are that the amplitude of the correlations are controlled by both the capacitance and the coupling constants with different ratios if we look at the dephasing or rephasing. The correlations get out of the range that our approximation allowed with quickly when varying a bit the coupling constants. Furthermore, to get the average value for the phase correlation, there is a time needed which increases with the distance at which we look at these correlations.
Further studies could continue to look at the "light-cone-like" effect in the dephasing and rephasing and the effect of a limited number of sites on it. Another important extension would be to include some sort of dissipation in the Hamiltonian. One could imagine to couple the JJA Hamiltonian to a thermal bath to include a temperature treatment, or include internal degrees of freedom at each site where the energy could go.

The second limit was a classical limit at finite temperature where we neglected the quantum terms and took box boundary conditions. We treated the system with a Langevin formalism (both analytically (with a linearization approximation) and numerically). We saw in a first time that the equilibrium values of the phase correlations where dictated by the ratio T/J, while the phenomenological parameter η controlled the time scale to reach the equilibrium. In a second time, we compared the predictions of our solution to an actual experiment done in cold dipolar gases and achieved a relatively good agreement and also showed the limitations of a "fixed-site"-JJA in the supersolid context of the experiment. This comparison is actually presented in [12]. Here, an interesting element to add to the model would be to be able to treat also a model where the sites of the JJA could move spatially and this would affect the Josephson coupling. We could then look at how the rephasing would occur with any given spatial oscillations and see the effects of a slow versus fast spatial oscillation of the sites.

Bibliography

[1] D. A. Abanin, E. Altman, I. Bloch, and M. Serbyn. Colloquium: Many-body localization, thermalization, and entanglement. *Rev. Mod. Phys.*, 91:021001, May 2019.

[2] T. Langen, R. Geiger, and J. Schmiedmayer. Ultracold atoms out of equilibrium. *Annu. Rev. Condens. Matter Phys.*, 6:201–217, March 2015.

[3] B. D. Josephson. Coupled superconductors. *Rev. Mod. Phys.*, 36:216–220, Jan 1964.

[4] M. Tinkham. *Introduction to Superconductivity.* McGraw-Hill, 2 edition, 1996.

[5] S.T. Herbert, L.B. Gomez, D.B. Mast, R.S. Newrock, C. Wilks, and C.M. Falco. Fabrication of 3d proximity coupled josephson junction arrays. *Superlattices and Microstructures*, 18:53–57, 1995.

[6] C. Bruder, R. Fazio, and G. Schon. The bose-hubbard model: from josephson junction arrays to optical lattices. *Annalen der Physik*, 14(9-10):566–577, August 2005.

[7] L. Foini and T. Giamarchi. Nonequilibrium dynamics of coupled luttinger liquids. *Phys. Rev. A*, 91:023627, Feb 2015.

[8] L. Foini and T. Giamarchi. Relaxation dynamics of two coherently coupled one-dimensional bosonic gases. *Eur. Phys. J. Special Topics*, 226:2763–2774, July 2017.

[9] S. Hofferberth, I. Lesanovsky, B. Fischer, T. Schumm, and J. Schmiedmayer. Non-equilibrium coherence dynamics in one-dimensional bose gases. *Nature*, 449:324–327, 2007.

[10] M. Cheneau, P. Barmettler, D. Poletti, M. Endres, P. Schauss, T. Fukuhara, G. Gross, I Bloch, C Kollath, and S. Kuhr. Light-cone-like spreading of correlations in a quantum many-body system. *Nature*, 481:484–487, Jan 2012.

[11] C. Kollath, A. M. Läuchli, and E. Altman. Quench dynamics and nonequilibrium phase diagram of the bose-hubbard model. *Phys. Rev. Lett.*, 98:180601, Apr 2007.

[12] P. Ilzhöfer, M. Sohmen, G. Durastante, C. Politi, A. Trautmann, G. Natale, G. Morpurgo, T. Giamarchi, L. Chomaz, G. Natale, M.J. Mark, and F. Ferlaino. Phase coherence in out-of-equilibrium supersolid states of ultracold dipolar atoms. *ArXiv:1912.10892*, 2019.

[13] T. Giamarchi. *Quantum Physics in One Dimension*, volume 121 of *International Series of Monographs on Physics*. Oxford Science Publications, Clarendon Press, Oxford, first edition, 2004.

[14] P. Ruggiero, T. Giamarchi, and L. Foini. Thermalization, prethermalization and impact of the temperature in the quench dynamics of two *unequal* luttinger liquids. *arXiv:2006.16088*, 2020.

[15] Thierry Giamarchi. Lecture notes on statistical field theory. https://dqmp.unige.ch/giamarchi/lecture-notes/, 2003.

[16] W.-C. Yueh. Eigenvalues of several tridiagonal matrices. *Applied Mathematics E-Notes [electronic only]*, 5:66–74, 2005.

[17] L. Chomaz, D. Petter, P. Ilzhöfer, G. Natale, A. Trautmann, C. Politi, G. Durastante, R. M. W. van Bijnen, A. Patscheider, M. Sohmen, M. J. Mark, and F. Ferlaino. Long-lived and transient supersolid behaviors in dipolar quantum gases. *Phys. Rev. X*, 9:021012, Apr 2019.

[18] P. B. Blakie, D. Baillie, L. Chomaz, and F. Ferlaino. Supersolidity in an elongated dipolar condensate. *arXiv:2004.12577*, 2020.

[19] Thierry Giamarchi, Anibal Iucci, and Cristophe Berthod. Introduction to many body physics. https://dqmp.unige.ch/giamarchi/local/people/thierry.giamarchi/, 2008-2013.

Appendices

Appendix A

Reminders of quantum mechanics

1 Quantum Harmonic Oscillator

Here is a brief reminder of the diagonalization of the quantum harmonic oscillator with the creation/destruction operators. With the Hamiltonian and also $\hbar = 1$:

$$H = \frac{\hat{p}^2}{2m} + \frac{1}{2}m\omega^2\hat{x}^2 \tag{A.1}$$

And with the transformation :

$$\begin{cases} a = \sqrt{\frac{m\omega}{2}}(\hat{x} + \frac{i}{m\omega}\hat{p}) & \hat{x} = \sqrt{\frac{1}{2m\omega}}(a^\dagger + a) \\ a^\dagger = \sqrt{\frac{m\omega}{2}}(\hat{x} + \frac{i}{m\omega}\hat{p}) & \hat{p} = i\sqrt{\frac{m\omega}{2}}(a^\dagger - a) \end{cases} \tag{A.2}$$

We get the diagonal form :

$$H = \omega(\frac{1}{2} + \sum_k a_k^\dagger a_k) \tag{A.3}$$

2 Evolution of a or b operator in time

The evolution of the operator a_k with the Hamiltonian H_{J_1} is given by [19]:

$$\frac{\mathrm{d}a_k(t)}{\mathrm{d}t} = ie^{iH_{J_1}t}[H_{J_1}, a_k]e^{-iH_{J_1}t} \tag{A.4}$$

with $H_{J_1} = \sum_k \frac{1}{2}\sqrt{\frac{2J_1}{C}(1-\cos(ka))}(a_k^\dagger a_k + a_k a_k^\dagger) = \sum_k \frac{1}{2}\omega_{1,k}(a_k^\dagger a_k + a_k a_k^\dagger)$, where we define ω as :

$$\omega_{1/2,k} = \sqrt{\frac{2J_{1/2}}{C}(1-\cos(ka))} \tag{A.5}$$

by computing the commutators $[a_k^\dagger a_k, a_q] = -a_q\delta_{k,q}$ and $[a_k a_k^\dagger, a_q] = -a_q\delta_{k,q}$, we get that $[H_{J_1}, a_k] = -\omega_{1,k}a_k$. This leads to :

$$\frac{\mathrm{d}a_k(t)}{\mathrm{d}t} = -i\omega_{1,k}a_k(t) \tag{A.6}$$

and by integrating, we get the expressions :

$$\begin{cases} a_k(t) = e^{-i\omega_{1,k}t} a_k \\ a_k^\dagger(t) = e^{i\omega_{1,k}t} a_k^\dagger \end{cases} \tag{A.7}$$

The crucial point is that H_{J_1} is quadratic in the a operators.

Equivalently, if we make evolve the b operators with H_{J_2}, we get :

$$\begin{cases} b_k(t) = e^{-i\omega_{2,k}t} b_k \\ b_k^\dagger(t) = e^{i\omega_{2,k}t} b_k^\dagger \end{cases} \tag{A.8}$$

Appendix B

Full quantum approach

1 Computation of $\langle\Psi(t_1)|\,\delta\theta_k\delta\theta_{k'}\,|\Psi(t_1)\rangle$

With (3.25), and the definition of $B_{1,k}$, we use the relations between a and b (3.16), and with a bit of algebra this leads us to :

$$\begin{aligned}\delta\theta_{k,J_1}(t_1)\delta\theta_{k',J_1}(t_1) = B_{1,k}B_{1,k'}\Bigg[&\left(\sqrt[4]{\frac{J_1}{J_2}}\cos(\omega_{1,k}t_1) - i\sqrt[4]{\frac{J_2}{J_1}}\sin(\omega_{1,k}t_1)\right)b_k \\ &+\left(\sqrt[4]{\frac{J_1}{J_2}}\cos(\omega_{1,k}t_1) + i\sqrt[4]{\frac{J_2}{J_1}}\sin(\omega_{1,k}t_1)\right)b^\dagger_{-k}\Bigg](\cdots)_{k'}\end{aligned} \tag{B.1}$$

where $(\cdots)_{k'}$ means the same expression but in terms of k' instead of k.

When we look at $\langle\varnothing|_b\,\delta\theta_{k,J_1}(t_1)\delta\theta_{k',J_1}(t_1)\,|\varnothing\rangle_b$, the only term which survives is the one where we first create a particle and then destroy it to return to the vacuum, of the form :

$$\langle\varnothing|_b\,b_k b^\dagger_{-k'}\,|\varnothing\rangle_b = \delta_{k,-k'} \tag{B.2}$$

Because $B_{1,k}$ and $\omega_{1,k}$ are even in k, this leads to :

$$\begin{aligned}\langle\varnothing|_b\,\delta\theta_{k,J_1}(t_1)\delta\theta_{k',J_1}(t_1)\,|\varnothing\rangle_b &= B^2_{1,k}\left(\sqrt[4]{\frac{J_1}{J_2}}\cos(\omega_{1,k}t_1) - i\sqrt[4]{\frac{J_2}{J_1}}\sin(\omega_{1,k}t_1)\right)\cdot \\ &\quad\left(\sqrt[4]{\frac{J_1}{J_2}}\cos(\omega_{1,k}t_1) + i\sqrt[4]{\frac{J_2}{J_1}}\sin(\omega_{1,k}t_1)\right)\delta_{k,-k'} \\ &= B^2_{1,k}\left(\sqrt{\frac{J_1}{J_2}}\cos^2(\omega_{1,k}t_1) + \sqrt{\frac{J_2}{J_1}}\sin^2(\omega_{1,k}t_1)\right)\end{aligned} \tag{B.3}$$

And by replacing $B_{1,k}$, we end up with (3.27).

2 Computation of $\langle\Psi(t_2)|\,\delta\theta_k\delta\theta_{k'}\,|\Psi(t_2)\rangle$

By writing $t_{21} = t_2 - t_1$, we have that :

$$\langle\Psi(t_2)|\,\delta\theta_k\delta\theta_{k'}\,|\Psi(t_2)\rangle = \langle\Psi(t_1)|\,\delta\theta_k(t_{21})\delta\theta_{k'}(t_{21})\,|\Psi(t_1)\rangle \tag{B.4}$$

We can now write $\delta\theta_k$ in term of b operators because it evolves first with H_{J_2}. Writing $C_{2,k} = \frac{1}{\sqrt{2}}\frac{1}{\sqrt[4]{2J_2C(1-\cos(ka))}}$ leads to :

$$\delta\theta_k(t_{21})\delta\theta_{k'}(t_{21}) = C_{2,k}C_{2,k'}\left(e^{-i\omega_{2,k}t_{21}}b_k + e^{i\omega_{2,k}t_{21}}b^\dagger_{-k}\right)(\cdots)_{k'} \tag{B.5}$$

Now, we have to make the operators evolve along H_{J_1}. Therefore, we have to rewrite the b operators in term of a operators (3.16). After some algebra, we get :

$$\langle\Psi(t_2)|\,\delta\theta_k\delta\theta_{k'}\,|\Psi(t_2)\rangle = C_{2,k}C_{2,k'}\,\langle t_1|\,\Omega_k\Omega_{k'}\,|t_1\rangle \tag{B.6}$$

where :

$$\Omega_k = A_{k,t_{21}}a_k + A^*_{k,t_{21}}a^\dagger_{-k} \tag{B.7}$$

and :

$$A_{k,t_{21}} = \sqrt[4]{\frac{J_2}{J_1}}\cos(\omega_{2,k}t_{21}) - i\sqrt[4]{\frac{J_1}{J_2}}\sin(\omega_{2,k}t_{21}) \tag{B.8}$$

We then can apply the time evolution with H_{J_1} :

$$\langle\Psi(t_2)|\,\delta\theta_k\delta\theta_{k'}\,|\Psi(t_2)\rangle = C_{2,k}C_{2,k'}\,\langle\varnothing|_b\,\Theta_k\Theta_{k'}\,|\varnothing\rangle_b \tag{B.9}$$

where :

$$\Theta_k = A_{k,t_{21}}e^{-i\omega_{2,k}t_{21}}a_k + A^*_{k,t_{21}}e^{i\omega_{2,k}t_{21}}a^\dagger_{-k} \tag{B.10}$$

Finally, we have to apply our operators to the vacuum of the b operators. Therefore, we have to change back the a to b operators. We end up with :

$$\begin{aligned}\Theta_k = A_{k,t_{21}}e^{-i\omega_{2,k}t_{21}}&\left[\frac{1}{2}\left(\sqrt[4]{\frac{J_2}{J_1}} + \sqrt[4]{\frac{J_1}{J_2}}\right)b_k + \frac{1}{2}\left(\sqrt[4]{\frac{J_1}{J_2}} - \sqrt[4]{\frac{J_2}{J_1}}\right)b^\dagger_{-k}\right]\\ &+ A^*_{k,t_{21}}e^{i\omega_{2,k}t_{21}}\left[\frac{1}{2}\left(\sqrt[4]{\frac{J_2}{J_1}} + \sqrt[4]{\frac{J_1}{J_2}}\right)b^\dagger_{-k} + \frac{1}{2}\left(\sqrt[4]{\frac{J_1}{J_2}} - \sqrt[4]{\frac{J_2}{J_1}}\right)b_k\right]\end{aligned} \tag{B.11}$$

$$\langle\Psi(t_2)|\,\delta\theta_k\delta\theta_{k'}\,|\Psi(t_2)\rangle = C_{2,k}C_{2,k'}\,\langle\varnothing|_b\,\Theta_k\Theta_{k'}\,|\varnothing\rangle_b \tag{B.12}$$

We know that only the term with $\langle\varnothing|_b\,b_kb^\dagger_{-k'}\,|\varnothing\rangle_b$ can survive. This leads to :

$$\begin{aligned}\langle\Psi(t_2)|\,\delta\theta_k\delta\theta_{k'}\,|\Psi(t_2)\rangle = C_{2,k}C_{2,k'}&\left[A_{k,t_{21}}\frac{e^{-i\omega_{2,k}t_{21}}}{2}\left(\sqrt[4]{\frac{J_2}{J_1}} + \sqrt[4]{\frac{J_1}{J_2}}\right) + A^*_{k,t_{21}}\frac{e^{i\omega_{2,k}t_{21}}}{2}\left(\sqrt[4]{\frac{J_1}{J_2}} - \sqrt[4]{\frac{J_2}{J_1}}\right)\right]\\ &\cdot[\cdots]_{k'}\,\langle\varnothing|_b\,b_kb^\dagger_{-k'}\,|\varnothing\rangle_b\end{aligned} \tag{B.13}$$

The last part of the computation is just algebra, but some quite nasty looking one. After a long simplification of the terms, we end up with the result written in (3.29).

3 Computation with a mass term to the phase fluctuations

In this case the Hamiltonian (3.1 becomes) :

$$H = \sum_{i=1}^{N} \frac{\delta n_i^2 a^2}{2C} + \sum_{i=1}^{N} \frac{J}{2}(\delta\theta_{i+1} - \delta\theta_i)^2 + \frac{m^2}{2}\delta\theta_i^2 \tag{B.14}$$

Using the same procedure as before, we get by a Fourier transform :

$$\sum_k \frac{a^2}{2C}\delta n_k^\dagger \delta n_k + \sum_k \frac{2J(1-\cos(ka)) + m^2}{2}\delta\theta_k^\dagger \delta\theta_k \tag{B.15}$$

And then, by indentifying again $\delta\theta_k$ to $\hat{x}$ and $a\delta n_k$ to $\hat{p}$. We then have to identify $\frac{1}{C}$ to m and $\frac{(2J(1-\cos(ka))+m^2)}{C}$ to ω^2.

The only difference here is the definition of ω, because $2J(1-\cos(ka))$ became $2J(1-\cos(ka)) + m^2$. Therefore, with exactly the same steps and only this difference, we get the diagonal Hamiltonian :

$$H = \sum_k \frac{1}{2}\sqrt{\frac{2J}{C}(1-\cos(ka)) + \frac{m^2}{C}}(b_k^\dagger b_k + b_k b_k^\dagger) \tag{B.16}$$

Then, we have to find the new relations between the operators a and b. Again, using the same steps, we get :

$$\begin{cases} \frac{1}{\sqrt{2}}\frac{1}{\sqrt[4]{2J_1C(1-\cos(ka))+m^2C}}(a_k + a_{-k}^\dagger) = \delta\theta_k = \frac{1}{\sqrt{2}}\frac{1}{\sqrt[4]{2J_2C(1-\cos(ka))+m^2C}}(b_k + b_{-k}^\dagger) \\ -\frac{i}{2}\frac{\sqrt[4]{2J_1C(1-\cos(ka))+m^2C}}{a}(a_k - a_{-k}^\dagger) = \delta n_k = -\frac{i}{2}\frac{\sqrt[4]{2J_2C(1-\cos(ka))+m^2C}}{a}(b_k - b_{-k}^\dagger) \end{cases} \tag{B.17}$$

And here we cannot simplify as much as before. But instead, if we define $\gamma_i = 2J_iC(1-\cos(ka)) + m^2C$, we get exactly the same expressions as before where J_i became γ_i.

From this, we conclude that all the formulas we got without the mass term are valid if we replace $2J(1-\cos(ka))$ by $2J(1-\cos(ka)) + m^2$, the ratios $\frac{J_1}{J_2}$ by $\frac{\gamma_1}{\gamma_2}$ and the new definition of ω.

The only thing which has yet to be discussed is the value of the mass term. For this, what the idea is that one can fix m such that the correlation $\left\langle(\delta\theta_{j_1} - \delta\theta_{j_2})^2\right\rangle$ has a mean value (without the oscillations) smaller than π^2. And from this one can look at the phase evolution when one quenches for the second time the system.

4 Computation with box boundary conditions

With box boundary conditions, our Hamiltonian becomes :

$$H = \sum_{i=1}^{N} \frac{\delta n_i^2 a^2}{2C} + \sum_{i=1}^{N-1} \frac{J}{2}(\delta\theta_{i+1} - \delta\theta_i)^2 \tag{B.18}$$

The main difference with the periodic boundary conditions is the transformation which diagonalizes the hamiltonian. In this case, we use a result of a mathematical paper [16], theorem 4. We suspect that there is a typo of a minus sign in the paper.

After normalisation of the eigenvectors, we get that the transformations are :

$$\begin{cases} \delta\tilde{\theta}_k = \sum_{n=1}^{N} \sqrt{\frac{2}{N}}(-1)^{n-1} \sin\left(\frac{k(2n-1)\pi}{2N}\right) \delta\theta_n & k \in [\![1, N-1]\!] \\ \delta\tilde{\theta}_k = \sum_{n=1}^{N} \sqrt{\frac{1}{N}}(-1)^{n-1} \sin\left(\frac{(2n-1)\pi}{2}\right) \delta\theta_n & k = N \\ \delta\theta_n = \sum_{k=1}^{N-1} \sqrt{\frac{2}{N}}(-1)^{n-1} \sin\left(\frac{k(2n-1)\pi}{2N}\right) \delta\theta_k + sqrt\frac{1}{N}(-1)^{n-1} \sin\left(\frac{(2n-1)\pi}{2}\right) \delta\theta_{k=N} \end{cases} \tag{B.19}$$

The first 2 transformations arise from the paper [16], while the third one can be checked by manually inserting the expressions for $\delta\tilde{\theta}_k$ in it and doing some algebra.

The Hamiltonian after transformation is :

$$\sum_k \frac{a^2}{2C} \delta\tilde{n}_k \delta\tilde{n}_k + J \sum_k (1 + \cos(\frac{k\pi}{N})) \delta\tilde{\theta}_k \delta\tilde{\theta}_k \tag{B.20}$$

To diagonalize this, we follow the same procedure following the resolution of the quantum harmonic oscillator.

Note that here k does not refer to a Fourier mode but to a mode of this transformation. The computation of the correlations $\left\langle \delta\tilde{\theta}_k \delta\tilde{\theta}_{k'} \right\rangle$ are exactly the same except for the factor $1 - \cos(ka)$ in the diagonal Hamiltonian which becomes here $1 - \cos(\frac{k\pi}{N})$. We get :

$$\left\langle \delta\tilde{\theta}_k \delta\tilde{\theta}_{k'} \right\rangle = C\delta_{k,k'} \tag{B.21}$$

where C is the coefficient found before the Kronecker delta in the periodic boundary case.

The only other difference is the expression of $\left\langle (\delta\tilde{\theta}_i - \delta\tilde{\theta}_j)^2 \right\rangle$ in terms of $\left\langle \delta\tilde{\theta}_k \delta\tilde{\theta}_{k'} \right\rangle$ which is (after some algebra) :

$$\left\langle (\delta\tilde{\theta}_i - \delta\tilde{\theta}_j)^2 \right\rangle = \sum_{k=1}^{N-1} \left[\frac{2}{N} \sin\left(\frac{k(2i-1)\pi}{2N}\right) - (-1)^{j-i} \sin\left(\frac{k(2j-1)\pi}{2N}\right) \right]^2 \left\langle \delta\tilde{\theta}_k \delta\tilde{\theta}_k \right\rangle \tag{B.22}$$

We can also add easily the mass term in this treatment by doing the same steps as before.

Appendix C

Classical approach

1 Computation of the normalization of the eigenvectors

The eigenvectors are given by :

$$u_j^{(k)} = \cos(\frac{(k-1)\pi(2j-1)}{2N}) \qquad k \in [\![1, N]\!], j \in [\![1, N]\!] \tag{C.1}$$

We now want to compute $\| u^{(k)} \|^2$ in order to normalize the eigenvectors.

If $k = 1$, $u_j^{(k)} = 1$. Hence, $\| u^{(k)} \|^2 = N$, and we get $u_{j\,\text{normalized}}^{(k=1)} = \frac{1}{\sqrt{N}}$.

If $k \neq 1$, we have :

$$\begin{aligned}
\| u^{(k)} \|^2 &= \sum_j \cos^2\left(\frac{(k-1)(2j-1)\pi}{2N}\right) = \sum_j \frac{1}{2} + \frac{1}{2}\cos\left(\frac{(k-1)(2j-1)\pi}{N}\right) \\
&= \frac{N}{2} + \frac{1}{4}\sum_{j=1}^{N} e^{i\frac{(k-1)\pi(2j-1)}{N}} + \frac{1}{4}\sum_{j=1}^{N} e^{-i\frac{(k-1)\pi(2j-1)}{N}} \\
&= \frac{N}{2} + \frac{1}{4}e^{-i\frac{(k-1)\pi}{N}}\sum_{j=1}^{N}\left(e^{i\frac{(k-1)\pi 2}{N}}\right)^j + \frac{1}{4}e^{i\frac{(k-1)\pi}{N}}\sum_{j=1}^{N}\left(e^{-i\frac{(k-1)\pi 2}{N}}\right)^j \\
&= \frac{N}{2} + \frac{1}{4}e^{-i\frac{(k-1)\pi}{N}}\frac{e^{i\frac{(k-1)\pi 2}{N}} - e^{i\frac{(k-1)\pi 2}{N}(N+1)}}{1 - e^{i\frac{(k-1)\pi 2}{N}}} + \frac{1}{4}e^{i\frac{(k-1)\pi}{N}}\frac{e^{-i\frac{(k-1)\pi 2}{N}} - e^{-i\frac{(k-1)\pi 2}{N}(N+1)}}{1 - e^{-i\frac{(k-1)\pi 2}{N}}} \\
&= \frac{N}{2} + \frac{1}{4}\frac{e^{i\frac{(k-1)\pi}{N}} - e^{i(k-1)\pi 2}e^{i\frac{(k-1)\pi}{N}}}{1 - e^{i\frac{(k-1)\pi 2}{N}}} + \frac{1}{4}\frac{e^{-i\frac{(k-1)\pi}{N}} - e^{-i(k-1)\pi 2}e^{-i\frac{(k-1)\pi}{N}}}{1 - e^{-i\frac{(k-1)\pi 2}{N}}} \\
&= \frac{N}{2} + \frac{1}{4}\frac{e^{i\frac{(k-1)\pi}{N}} - e^{i\frac{(k-1)\pi}{N}}}{1 - e^{i\frac{(k-1)\pi 2}{N}}} + \frac{1}{4}\frac{e^{-i\frac{(k-1)\pi}{N}} - e^{-i\frac{(k-1)\pi}{N}}}{1 - e^{-i\frac{(k-1)\pi 2}{N}}} \\
&= \frac{N}{2}
\end{aligned} \tag{C.2}$$

where we used the formula for a geometric serie and then almost everything cancelled out.

We then get indeed that : $u_{j\,\text{normalized}}^{(k\neq 1)} = \frac{2}{\sqrt{N}}\cos(\frac{(k-1)\pi(2j-1)}{2N})$